AD_____

Award Number: W81XWH-05-1-0011

TITLE: Enhancement of Anti-telomerase Immunity against Prostate Cancer

PRINCIPAL INVESTIGATOR: Johannes Vieweg, M.D.

CONTRACTING ORGANIZATION: Duke University Medical Center
Durham, NC 27710

REPORT DATE: November 2007

TYPE OF REPORT: Annual

PREPARED FOR: U.S. Army Medical Research and Materiel Command
Fort Detrick, Maryland 21702-5012

# REPORT DOCUMENTATION PAGE

*Form Approved*
*OMB No. 0704-0188*



| **1. REPORT DATE** | **2. REPORT TYPE** | **3. DATES COVERED** |
|---|---|---|
| 14-11-2007 | Annual | 15 Oct 2006 – 14 Oct 2007 |

**4. TITLE AND SUBTITLE**

Enhancement of Anti-telomerase Immunity against Prostate Cancer

**5a. CONTRACT NUMBER**

**5b. GRANT NUMBER**
W81XWH-05-1-0011

**5c. PROGRAM ELEMENT NUMBER**

**6. AUTHOR(S)**

Johannes Vieweg, M.D.

Email: j.vieweg@urology.ufl.edu

**5d. PROJECT NUMBER**

**5e. TASK NUMBER**

**5f. WORK UNIT NUMBER**

**7. PERFORMING ORGANIZATION NAME(S) AND ADDRESS(ES)**

Duke University Medical Center
Durham, NC 27710

**8. PERFORMING ORGANIZATION REPORT NUMBER**

**9. SPONSORING / MONITORING AGENCY NAME(S) AND ADDRESS(ES)**
U.S. Army Medical Research and Materiel Command
Fort Detrick, Maryland 21702-5012

**10. SPONSOR/MONITOR'S ACRONYM(S)**

**11. SPONSOR/MONITOR'S REPORT NUMBER(S)**

**12. DISTRIBUTION / AVAILABILITY STATEMENT**
Approved for Public Release; Distribution Unlimited

**13. SUPPLEMENTARY NOTES**

**14. ABSTRACT**

NOT PROVIDED

**15. SUBJECT TERMS**
Prostate Cancer

| **16. SECURITY CLASSIFICATION OF:** | | | **17. LIMITATION OF ABSTRACT** | **18. NUMBER OF PAGES** | **19a. NAME OF RESPONSIBLE PERSON** |
|---|---|---|---|---|---|
| **a. REPORT** | **b. ABSTRACT** | **c. THIS PAGE** | | | USAMRMC |
| U | U | U | UU | 47 | **19b. TELEPHONE NUMBER** *(include area code)* |

# TABLE OF CONTENTS

**PAGE**

**"Enhancement of Anti-Telomerase Immunity against Prostate Cancer"**

**W81XWH-05-1-0011 (PI Johannes Vieweg, M.D.)**

**Annual Report 2007/2008**

## INTRODUCTION

The major objective of this proposal is to enhance the efficacy of specific active immunotherapy (SAI) by selectively eliminating or reducing $CD4^+$ regulatory T cells ($T_{reg}$)[1] in patients with metastatic prostate cancer. Preclinical and clinical data from our laboratory have shown that $CD4^+$ and $CD25^+$ co-expressing $T_{reg}$ play an important role in the suppression of T cell responses in the cancer patient. Moreover, we have demonstrated that elimination of $T_{reg}$ is capable of enhancing T-cell proliferation and cytolytic activity *in vitro.*[2]

A recent report previously suggested that human $T_{reg}$ can selectively be depleted in cancer patients using the IL-2/diphtheria toxin conjugate denileukin diftitox,[3] without inducing toxicity on other cellular subsets with intermediate or low expression of CD25. Most importantly, denileukin diftitox-mediated elimination of $T_{reg}$ followed by vaccination with tumor RNA-transfected DC significantly improved the stimulation of tumor-specific T-cell responses in RCC patients, when compared to vaccination alone (**Appendix A**). Cumulatively, these findings formed the basis of performing a clinical study in which the $T_{reg}$ depletion strategy was tested in patients with metastatic prostate cancer.

## BODY

A clinical trial was performed at Duke University Medical Center (IRB # 5278-05-10R2) enrolling a total of 15 patients with metastatic prostate adenocarcinoma, stage ($T_{1-4}$, N+, $M_0$) or ($T_{1-4}$, $N_{0-1}$, M+). Due to the PI's relocation to UF, the trial was closed in June 2006. All patients have undergone leukapheresis and were treated in this Institutional Review Board (IRB) and Food and Drug Administration (FDA)-approved study. From all study subjects it was possible to produce the vaccine consisting of LAMP TERT mRNA-transfected DC, according FDA-approved protocols (BB-IND 10036). Six subjects, enrolled on dose Schedule A, treatment arm A, received a single intravenous dose of denileukin diftitox (18µg/kg) four days prior to vaccination with LAMP hTERT mRNA-transfected DC, while a second cohort (Treatment arm B) of 6 subjects was treated with the vaccine alone. Treatment on both study arms was generally well tolerated with only one adverse event (grade III anemia, likely tumor mediated) reported to regulatory agencies. Two patients were treated on dose Schedule B treatment arm A (n=1) and B (n=1). In one patient there was progression of disease following the third vaccination and was therefore withdrawn from treatment. Although the targeted goal of enrollment into this trial was 24 patients, we collected sufficient data to support the primary endpoint, namely vaccine safety, of this regimen.

### *Analysis of regulatory T cells in the peripheral blood of prostate cancer patients.*

At UF, we started analyzing $T_{reg}$ frequencies in the peripheral blood of study patients collected prior to and after denileukin diftitox administration. Specifically, PBMC were collected from all subjects prior to (Pre ONT), four days after denileukin diftitox administration (Post ONT), and one month after vaccine treatment (Post vaccine). For in vivo $T_{reg}$ identification and tracking, CD4 positive T-cells were isolated from the PBMC of study patients by magnetic bead separation, then stained with CD25 or FoxP3 antibodies, and finally analyzed for the presence of triple positive $T_{reg}$ using flow cytometry.

As shown in **Figure 1** and **Table 1**, denileukin diftitox administration resulted in a significant, albeit modest reduction of $CD4^+/CD25^{high}/FoxP3^+$ triple positive $T_{reg}$ in 5/6 patients treated in the denileukin diftitox arm. As observed previously, $T_{reg}$ nadir was reached as early as 4 days after denileukin diftitox administration.

While we were pleased with the consistency and reproducibility of these experimental results, it was apparent that baseline $T_{reg}$ levels in metastatic prostate cancer patients were significantly lower (approximately 60.5%) that those observed in metastatic renal cell carcinoma patients (**Appendix A**). This is constant with other reports demonstrating disease-specific variability of $T_{reg}$ levels in the peripheral blood of melanoma, renal cell and ovarian carcinoma patients. Furthermore and in contrast to our prior experience in RCC patients, $T_{reg}$ depletion levels after denileukin diftitox administration were significantly inferior in prostate cancer patients when compared to RCC.

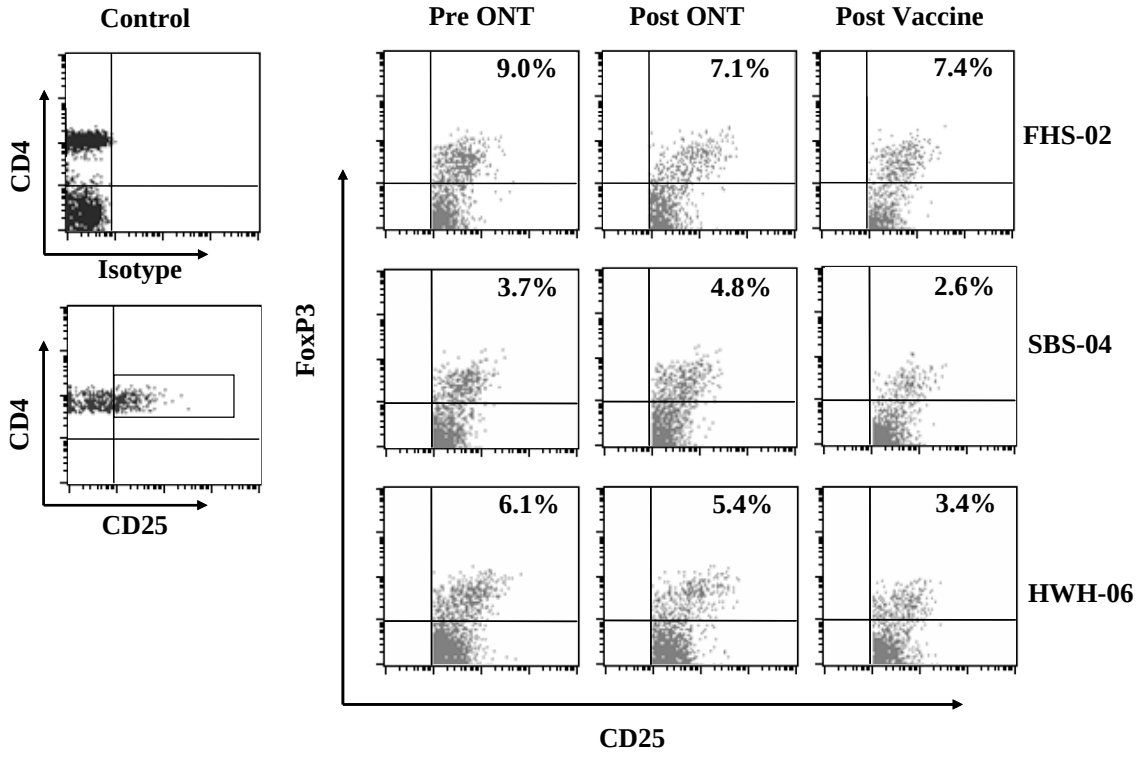


**Figure 1. Depletion of $CD4^+/CD25^+/FoxP3^+$ $T_{reg}$ in patients with metastatic prostate cancers.** Peripheral blood samples (PBMC) were collected from 3 study subjects who received a single dose of denileukin diftitox (18µg/kg). PBMC were collected prior to (Pre ONT), four days after denileukin diftitox administration (Post ONT), and one month after denileukin diftitox administration (Post vaccine). To quantitate $T_{reg}$ in peripheral blood samples, CD4+ T-cells were first isolated from PBMC by magnetic bead separation, then stained with CD25 or FoxP3 antibodies, and finally analyzed for the presence of triple positive $T_{reg}$ using flow cytometry. The results obtained from 3 subjects are shown.

**Table 1. Treg depletion levels after denileukin diftitox administration in 6 patients with metastatic prostate carcinoma.**

| Patient ID | Treg Pre Ontak | Treg Post Ontak | Treg Depletion level [%] |
|---|---|---|---|
| 01 | 2.9 | 2.5 | - 13.8% |
| 02 | 9.0 | 7.1 | - 21.1% |
| 03 | 2.5 | 2.3 | - 8.0% |
| 04 | 3.7 | 4.8 | + 29.7% |
| 05 | 3.3 | 3.2 | - 3.0 |
| 06 | 6.1 | 5.4 | -11.5 |

***Immunological analysis of $T_{reg}$ depleted PBMC.***

In order to determine vaccine-induced stimulation of hTERT-specific T-cell responses in the 6 subjects treated with denileukin diftitox followed by vaccination with hTERT mRNA transfected DC, we analyzed and compared directly the numbers of hTERT-specific T cells from pre- and post-therapy PBMC samples using ELISPOT analysis.

In preparation for this trial, we have previously developed a modified Interferon-γ spot assay, in which mRNA-transfected DC were used as targets for *in vitro* antigenic stimulation: Aliquots of PBMC obtained at baseline and 2 weeks after the sixth vaccination were thawed, T cells were isolated by negative depletion and cultured overnight with DC that had been transfected with hTERT or LAMP-hTERT mRNA. As controls, unloaded DC (data not shown) or green fluorescent protein (GFP) mRNA-transfected DC were used as stimulators. As shown in Figure 2, the numbers of hTERT-specific IFN-γ secreting cells was expectedly low or undetectable when T cells isolated from pre-therapy PBMC samples were analyzed, while after vaccination all 2 patients exhibited significant expansion of hTERT-specific T cells. The magnitude of the observed increases in the numbers of hTERT-specific T cells following vaccination is notable in view of the fact that analysis was performed directly from peripheral blood cells without the need for repeated *in vitro* restimulations. In stark contrast, no reactivity was observed against unloaded DC (not shown) or DC transfected with GFP RNA in any PBMC sample obtained from study subjects prior or post vaccination.

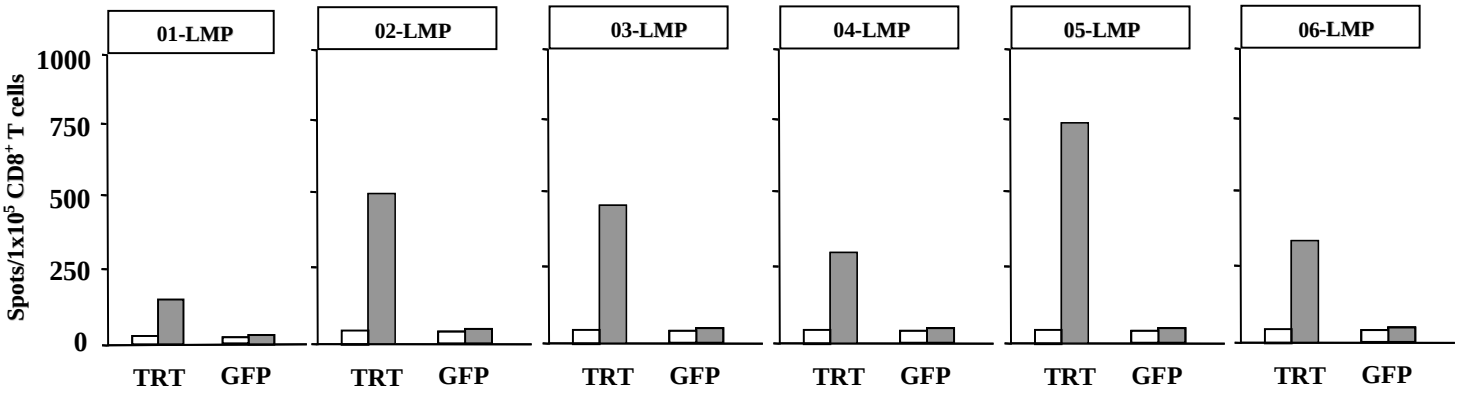


**Figure 2. T-cell induction after Treg depletion and vaccination with LAMP hTERT mRNA-transfected DC.** PBMC from pre- and post vaccination peripheral blood samples were incubated overnight with hTERT mRNA loaded DC (targets) as demonstrated in the text. Following short-term antigenic stimulation (using RNA transfected DC), cells were plated onto IFN-γ capture antibody-coated nitrocellulose plates. Visible spots were enumerated using an automated ELISPOT reader. As control targets either unloaded DC (DC) or GFP RNA loaded DC were used (data not shown).

**The data shown above suggest successful stimulation of hTERT-specific T cells in the peripheral blood of the 6 patients treated with denileukin diftitox and the hTERT vaccine. Studies are ongoing to determine and compare hTERT-specific T-cell responses from patients enrolled in the vaccine only arm.**

***Detection of Myeloid suppressor cells in the peripheral blood of renal cancer patients.***

Previous studies have shown that not only $T_{reg}$ but other cellular subsets in prostate and renal cell carcinoma patients trigger profound immunosuppression in the tumor bearing host. Specifically, we and other have demonstrated the presence of a novel cellular subset, termed myeloid suppressor cells (MDSC), in patients with metastatic renal cell carcinoma (**Appendix B**). MDSC have shown to interfere with the differentiation, function

and survival of antigen presenting (APC) and effector T cells by utilizing enzymes involved in arginine metabolism, namely inducible nitric oxide synthase which generates nitric oxide, and arginase I, which acts by L-arginine depletion. Although several studies have analyzed the phenotype and function of MDSC in murine systems, much less is known regarding the relevance and immunosuppressive action of MDSC in cancer patients. Using peripheral blood of RCC patients as a substrate, we found that the frequencies of CD33+HLA-DR- MDSC isolated from the peripheral blood of patients with metastastic (RCC) are significantly elevated when compared to CD33+HLA-DR- cells from healthy donors (see **Figure 3**). Specifically, we isolated PBMC from RCC patients and control healthy donors and then analyzed for presence of lineage negative/HLA-DR negative cell populations (Lin-/DR-). As shown in Fig.3A and 3B, the number of Lin-HLA-DR- cells was significantly increased in cancer patients Subsequently, Lin-/DR- cells were analyzed for cell surface expression of CD1a, CD10, CD11b, CD13, CD114, CD18, CD31, CD33, HLA ABC and HLA-DR. As shown in Figure 1C, Lin-/DR- cells exhibited high expression levels of HLA class I, CD18, CD33, and intermediate cell surface expression for CD1a, CD10, CD13, CD31 and CD11b, consistent with the MDSC phenotype previously described.

Complementary studies (shown in **Appendix B**) were performed to demonstrate the immunosuppressive nature of these MDSC and their responsiveness to ATRA that abrogated their immunsuppressive phenotype in vitro.

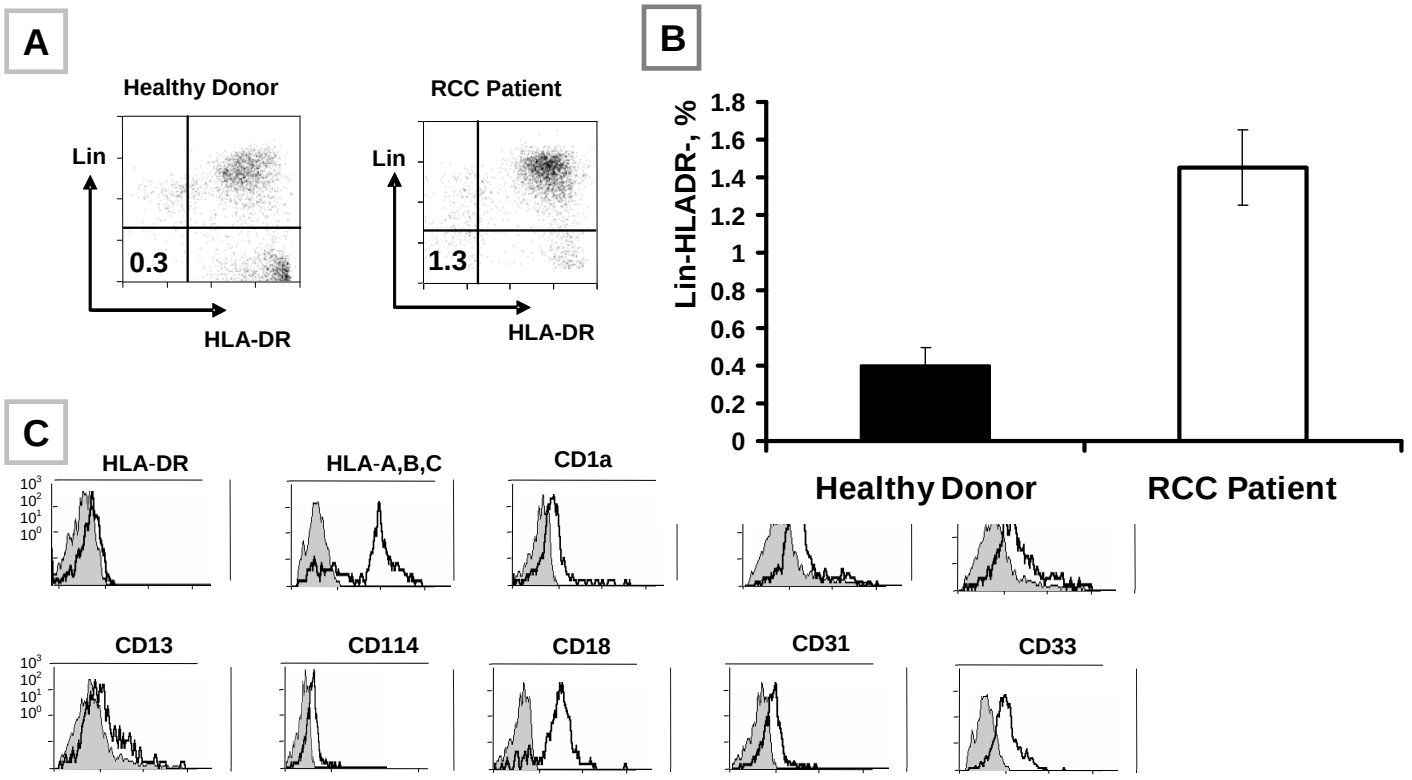


Fig.1

**Figure 3. Characterization of Lin$^-$HLA-DR$^-$ myeloid cell population in peripheral blood of RCC patients.** **A**. MDSC were isolated from the PBMC of healthy donors and RCC patients (One representative pair of donor-patient from 9 are shown) by selecting lineage negative (CD3, CD14, CD19, CD56) and HLA-DR negative cells as described previously [4]. **B.** Proportion of Lin$^-$HLA-DR$^-$ cells in peripheral blood of RCC patients is significantly increased. Freshly isolated PBMC from RCC patients and healthy donors were stained with CD3, CD14, CD19, CD56 and HLA-DR, and then analyzed by flow cytometry for presence of Lin$^-$HLA-DR$^-$ cell population. **C.** Lin$^-$HLA-DR$^-$ MDSC populations were characterized by flow cytometry. Cell surface marker expression is represented by the white histograms, while isotype controls are shown in the gray histograms.

## KEY RESEARCH ACCOMPLISHMENTS

a) Successful translation of the $T_{reg}$ depletion concept into the clinic by executing a complex phase I/II study and treating study subjects with a combined $T_{reg}$ depletory/vaccine regimen.

b) Preliminary data suggest that administration of a single dose of denileukin diftitox (18µg/kg) is capable of selectively eliminating CD25-expressing regulatory T cell subsets from the PBMC of prostate cancer patients.

c) $T_{reg}$ baseline levels in metastatic prostate cancer patients are significantly inferior to those observed in the peripheral blood of metastatic RCC patients (see **Appendix A**)

d) Denileukin diftitox-mediated $T_{reg}$ depletion was less effective than in patients with metastatic RCC

e) Immune analysis demonstrated significant expansion of hTERT-specific T cells in the peripheral blood of vaccine candidates after $T_{reg}$ depletion. Further experiments are underway to provide more an in depth analysis on the vaccine-mediated T-cell response by characterizing their functional ability to lyse tumor cells and determine the exact phenotype and cytokine profiles of vaccine-induced $CD4^+$ and $CD8^+$ T-cell subsets.

f) Myeloid suppressor cells can be identified in the peripheral blood of cancer patients. These cells are profoundly immunosuppressive by inhibiting T-cell function.

g) MSDC-mediated immunosuppression could be inhibited through exposure to the differentiation agent ATRA (all-tran retinoic acid).

## REPORTABLE OUTCOMES


1. Dannull, J., Kusmartsev, S., Su, Z., Heiser, A., Kubler, H., Yancey, D., Coleman, D., Vieweg, J.,: *Reversal of Myeloid $CD33^+$ Cell-mediated Immunosuppression in Patients with Metastatic Renal Cell Carcinoma*. Clinical Cancer Research. In press.
2. Kusmartsev, S., Eruslanov, E., Kubler, H., Tseng, T., Sakai, Y., Su, Z., Kaliberov, S., Rosser, C., Dahm, P., Vieweg, J.: *Presence of Tumor-Enduced VEGFR1+CD11b+ Myeloid Cells in Cancer Patients with Metastatic Renal Cell Carcinoma: Link to Immune Suppression and Angiogenesis*. Clinical Cancer Reserch. In press.
3. **Vieweg, J**., Su, Z., Dahm, P. & Kusmartsev, S.: *Reversal of Tumor-Mediated Immunosuppression*. Clin Cancer Res 2007, Jan 15;13:727s-732s.
4. **Vieweg, J**. *Immunotherapy for Advanced Prostate Cancer*. Rev Urol 2007; 9 Supp 1: S29-S38
5. **Vieweg, J**. *The evolving therapeutic landscape of prostate cancer*. Curr Opin Urol 2007;17:156


## CONCLUSIONS

We have madder considerable progress in the analysis of a complex phase I/II study that will serve as a basis for subsequent phase II clinical trials that would receive input specifications arising from the biologic and clinical results of this ongoing phase I trial.

## REFERENCES


1. Shevach, E.M., *Certified professionals: CD4(+)CD25(+) suppressor T cells.* J Exp Med, 2001. **193**(11): p. F41-6.
2. Dannull, J., et al., *Enhancement of vaccine-mediated antitumor immunity in cancer patients after depletion of regulatory T cells.* J Clin Invest, 2005. **115**(12): p. 3623-33.
3. Frankel, A.E., et al., *Chimeric fusion proteins--diphtheria toxin-based.* Curr Opin Investig Drugs, 2001. **2**(9): p. 1294-301.
4. Almand, B., et al., *Increased production of immature myeloid cells in cancer patients. A mechanism of immunosuppression in cancer.* J. Immunol, 2001. **166**(1): p. 678-689.


## APPENDICES

1. Dannull, J., et al., *Enhancement of vaccine-mediated antitumor immunity in cancer patients after depletion of regulatory T cells*.
2. Kustmartsev, S., et al., *Reversal of myeloid cell-mediated immunosuppression in patients with metastatic renal cell carcinoma*.

# Appendices A

# Enhancement of vaccine-mediated antitumor immunity in cancer patients after depletion of regulatory T cells

Jens Dannull,[1] Zhen Su,[1] David Rizzieri,[2] Benjamin K. Yang,[1] Doris Coleman,[1] Donna Yancey,[1] Aijing Zhang,[1] Philipp Dahm,[1] Nelson Chao,[2] Eli Gilboa,[1] and Johannes Vieweg[1]

[1]Genitourinary Cancer Immunotherapy Program, Division of Urology, Department of Surgery, and
[2]Division of Cellular Therapy, Department of Medicine, Duke University Medical Center, Durham, North Carolina, USA.

**In this study, we investigated whether elimination of $CD4^+/CD25^+$ Tregs using the recombinant IL-2 diphtheria toxin conjugate $DAB_{389}$IL-2 (also known as denileukin diftitox and ONTAK) is capable of enhancing the immunostimulatory efficacy of tumor RNA-transfected DC vaccines. We show that $DAB_{389}$IL-2 is capable of selectively eliminating CD25-expressing Tregs from the PBMCs of cancer patients without inducing toxicity on other cellular subsets with intermediate or low expression of CD25. $DAB_{389}$IL-2–mediated Treg depletion resulted in enhanced stimulation of proliferative and cytotoxic T cell responses in vitro but only when $DAB_{389}$IL-2 was omitted during T cell priming. $DAB_{389}$IL-2 significantly reduced the number of Tregs present in the peripheral blood of metastatic renal cell carcinoma (RCC) patients and abrogated Treg-mediated immunosuppressive activity in vivo. Moreover, $DAB_{389}$IL-2–mediated elimination of Tregs followed by vaccination with RNA-transfected DCs significantly improved the stimulation of tumor-specific T cell responses in RCC patients when compared with vaccination alone. Our findings may have implications in the design of immune-based strategies that may incorporate the Treg depletion strategy to achieve potent antitumor immunity with therapeutic impact.**

## Introduction

We have previously shown that vaccination with RNA-transfected DCs is an effective strategy to stimulate potent T cell responses in patients with metastatic cancers (1, 2). In this study, we investigated whether the immunostimulatory properties of RNA-transfected DC vaccines can be further enhanced by disrupting regulatory pathways that suppress the activation and function of tumor-specific T effector cells in the cancer patient. Recent research has shown that $CD4^+$ T cells constitutively expressing the IL-2 receptor α-chain (CD25) act in a regulatory capacity by suppressing the activation and function of other T cells (3). Their physiological role is to protect the host against the development of autoimmunity by regulating immune responses against antigens expressed by normal tissues (4, 5). Since tumor antigens are largely self antigens, Tregs may also prevent the tumor-bearing host from mounting an effective antitumor immune response. Previous studies have shown that elevated numbers of $CD4^+CD25^+$ Tregs can be found in advanced cancer patients (6) and that high Treg frequencies are associated with reduced survival (7). The important role of $CD4^+CD25^+$ Tregs in controlling tumor growth was further highlighted by the demonstration that depletion of Tregs using anti-CD25 antibodies can evoke effective antitumor immunity in mice (8, 9). Moreover, anti-CD25 therapy enhanced the therapeutic efficacy of GM-CSF–secreting B16 tumor cells and prolonged survival of tumor-bearing animals (10). Cumulatively, these experimental data suggest that the efficacy of cancer vaccination could be enhanced by treatment with agents that lead to the preferential depletion of $CD4^+CD25^+$ Tregs, such as compounds that target cells expressing the IL-2 receptor CD25 subunit.

In this study, we used the recombinant IL-2 diphtheria toxin conjugate $DAB_{389}$IL-2 (also known as denileukin diftitox and ONTAK) to eliminate CD25-expressing Tregs in metastatic renal cell carcinoma (RCC) patients. $DAB_{389}$IL-2 contains the catalytical and membrane translocation domain of diphtheria toxin (11). The binding domain for the diphtheria toxin receptor, however, is deleted and replaced by the human IL-2 gene, which allows for targeting of CD25-expressing cells. The cytotoxic action of $DAB_{389}$IL-2 occurs as a result of binding to the high-affinity IL-2 receptor, subsequent internalization, and enzymatic inhibition of protein synthesis, ultimately leading to cell death.

Here we show that $DAB_{389}$IL-2 is capable of selectively eliminating Tregs from human PBMCs in a dose-dependent manner without apparent bystander toxicity to other PBMCs or $CD4^+$ T cells with intermediate- or low-level expression of CD25. Treg depletion resulted in enhanced stimulation of proliferative and cytotoxic T cell responses in vitro but only when $DAB_{389}$IL-2 was used prior to and omitted during the T cell priming phase. Depletion of Tregs in RCC patients followed by vaccination with tumor RNA-transfected DCs led to improved stimulation of tumor-specific T cells when compared with vaccination alone. To our knowledge, we provide the first clinical evidence that in vivo elimination of Tregs is capable of enhancing the magnitude of vaccine-mediated, tumor-specific T cell responses in humans.

**Nonstandard abbreviations used:** 7-AAD, 7-amino-actinomycin D; CTLA-4, CTL-associated antigen-4; $DAB_{389}$IL-2, recombinant IL-2 diphtheria toxin conjugate; fluM1, influenza virus matrix protein 1; FoxP3, forkhead box P3 transcriptional regulator; GITR, glucocorticoid-induced TNF receptor family gene; hTERT, human telomerase reverse transcriptase; MART-1, melanocyte antigen recognized by T cells 1; MLR, mixed-lymphocyte reaction; MTT, 3-(4,5-dimethylthiazol-2-yl)-2,5-diphenyl tetrazolium bromide salt; OVA, ovarian carcinoma; RCC, renal cell carcinoma; RE, renal epithelium.

**Conflict of interest:** The authors have declared that no conflict of interest exists.

**Citation for this article:** *J. Clin. Invest.* **115**:3623–3633 (2005). doi:10.1172/JCI25947.

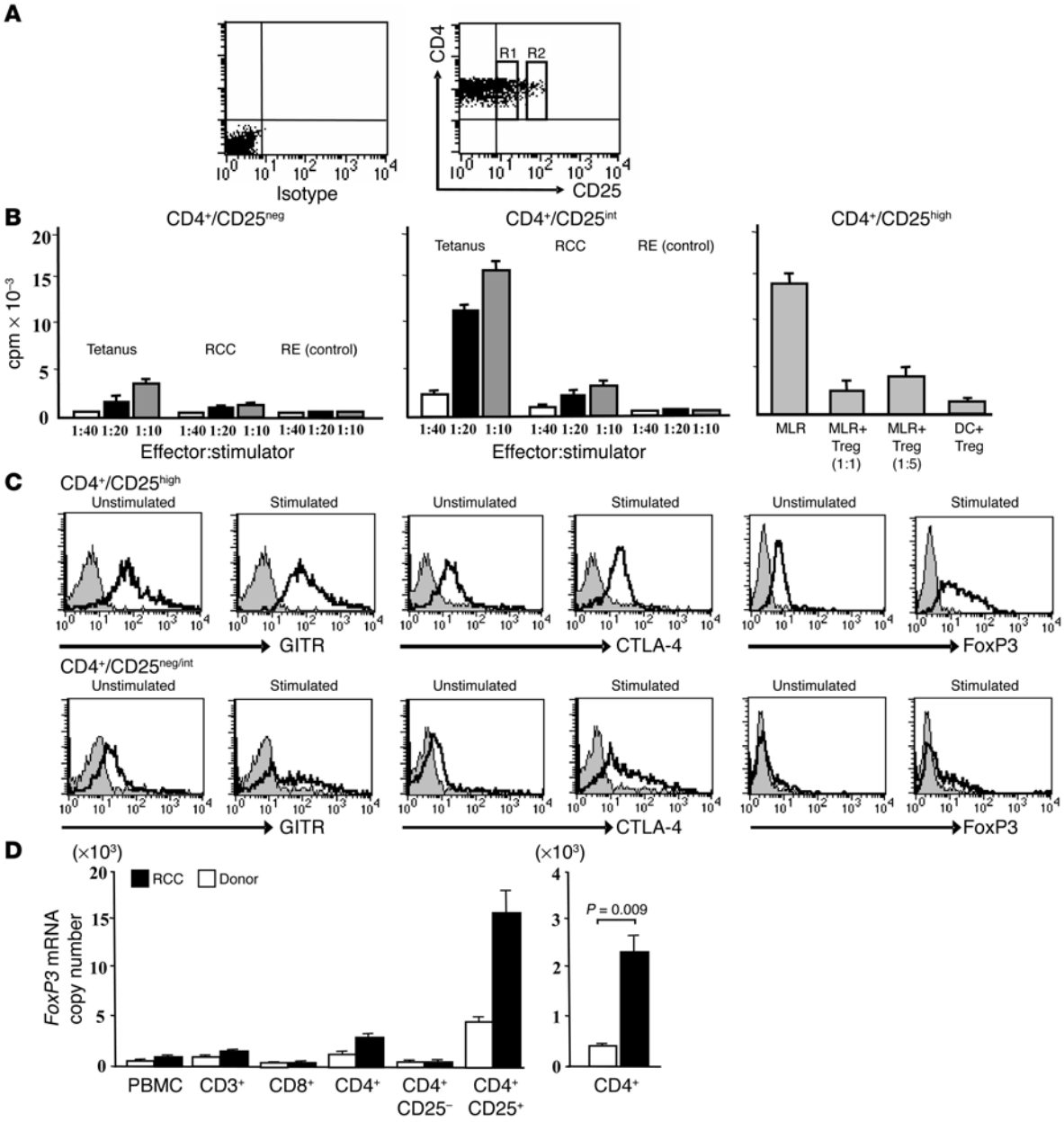


**Figure 1**

Characterization of CD4+ T cell subsets. (**A**) PBMCs from an RCC patient were stained with anti-CD4/CD25 mAbs and analyzed by FACS. (**B**) $CD4^+CD25^{neg}$, $CD4^+CD25^{int}$ (R1), and $CD4^+CD25^{high}$ (R2) T cells were sorted. For functional analysis, $CD4^+CD25^{neg}$ (left panel) and $CD4^+CD25^{int}$ (middle panel) T cells were stimulated with tetanus toxoid–loaded DCs (tetanus), DCs transfected with autologous RCC RNA (RCC), or with DCs transfected with autologous RE RNA (RE) at the indicated stimulator to responder ratios. After 48 hours, cells were pulsed with $^3$H-thymidine, and incorporation was determined using a liquid scintillation counter. $CD4^+CD25^{high}$ cells (right panel) were functionally validated by MLR. Mixture ratios of 1 $CD4^+CD25^{high}$ cell per T cell (Treg 1:1) or 1 $CD4^+CD25^{high}$ cell per 5 T cells (Treg 1:5) were added to the reaction, and inhibition of cell proliferation was analyzed. As a negative control, proliferation of $CD4^+CD25^{high}$ cells was determined in the presence of allogeneic DCs only (DC+Treg). Results are presented as means with SD calculated from triplicate wells. (**C**) FACS-based detection of GITR, CTLA-4, and FoxP3 by $CD4^+CD25^{neg/int}$ and $CD4^+CD25^{high}$ T cells subsets with or without stimulation using anti-CD3/CD28 mAb. Gray histograms represent isotypic controls. (**D**) Left panel: analysis of *FoxP3* transcripts was performed by real-time PCR on indicated T cell populations. *FoxP3* mRNA copy numbers were normalized to $1 \times 10^7$ copies of β-*actin* mRNA. A representative result from 3 subjects is shown. Right panel: *FoxP3* mRNA was amplified from $CD4^+$ T cells isolated from RCC patients ($n = 5$) and healthy donors ($n = 5$). Differences in *FoxP3* mRNA expression among groups were significant ($P = 0.009$).

## Results

*Phenotypic and functional characterization of Tregs.* The definition and enumeration of human Tregs is complicated by the fact that CD25 is a marker of T cell activation (12, 13). Human $CD4^+$ T cells expressing CD25 represent a heterogeneous cell population containing not only regulatory but also effector/memory

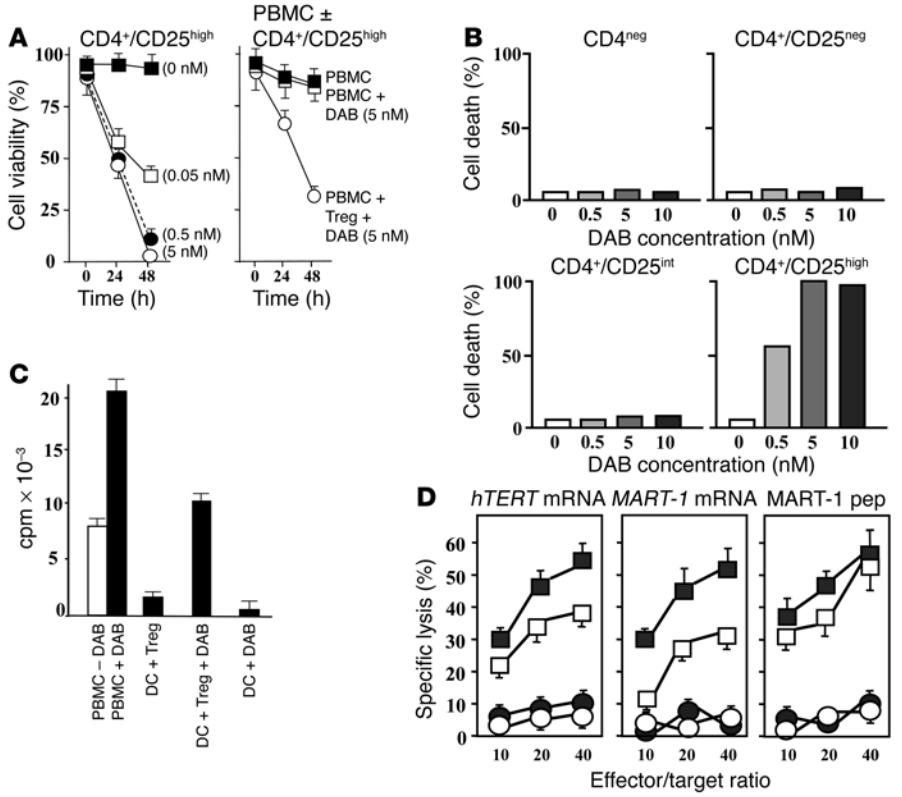


**Figure 2**
Enhancement of T cell responses after Treg depletion. (**A** and **B**) $CD4^+CD25^{high}$ cells were isolated by FACS sorting and incubated for 6 hours in the presence of increasing concentrations of $DAB_{389}$IL-2 (left panel). In order to determine $DAB_{389}$IL-2–mediated toxicity, PBMCs and PBMCs admixed with $CD4^+/CD25^{high}$ cells at a 1:1 ratio were incubated with or without $DAB_{389}$IL-2 (5 nM) for 6 hours. In all experiments, cell viability was determined through MTT assays (**A**) or 7-AAD staining (**B**). Representative results from 3 evaluable subjects are presented. (**C**) Treg-depleted PBMCs (PBMC+DAB) or nondepleted PBMCs (PBMC–DAB) from an RCC patient were analyzed in allogeneic MLRs using DCs at a responder to stimulator ratio of 20:1. Cell proliferation was significantly inhibited when isolated $CD4^+/CD25^{high}$ cells were added to PBMCs at a 1:1 PBMC/$CD4^+CD25^{high}$ cell ratio (DC+Treg). This inhibition was reversible when the added $CD4^+/CD25^{high}$ cells were pretreated with $DAB_{389}$IL-2 (5 nM) for 48 hours (DC+Treg+DAB). Exposure of PBMCs to $DAB_{389}$IL-2 during the T cell–priming phase (day 2) led to complete inhibition of T cell proliferation (DC+DAB). (**D**) DCs transfected with mRNA encoding *hTERT* or *MART-1* were used to stimulate CTL from Treg-depleted (filled symbols) or nondepleted (open symbols) human PBMCs.In addition, DCs loaded with MART-1–derived peptide 26-35 ELAGIGILTV (MART-1 pep) were used as stimulators. Following 2 stimulation cycles, CTLs were analyzed for their capacity to lyse their cognate (squares) or control targets (circles). As control targets, DCs loaded with *GFP* mRNA (mock transfected) or irrelevant peptide were used.

T cells (14). Analysis of PBMCs from healthy donors and RCC patients revealed the presence of $CD4^+$ T cell populations that express increasing levels of CD25 (14). As shown in Figure 1A, 1 major subset of $CD4^+$ T cells, isolated from the PBMCs of an RCC patient, lacked CD25 expression while a second population was characterized by intermediate levels of CD25, and a third, albeit small portion, exhibited high CD25 cell surface expression levels. To further characterize these 3 subsets, $CD4^+/CD25^{neg}$, $CD4^+/CD25^{int}$, and $CD4^+/CD25^{high}$ T cells were isolated from the PBMCs of RCC patients by FACS and functionally analyzed in vitro (Figure 1B). $CD4^+/CD25^{neg}$ cells expressed cell surface markers characteristic of naive/resting T cells and demonstrated reduced proliferative activity following exposure to tetanus toxoid, renal tumor RNA, benign renal epithelium (RE) RNA, and PBMC RNA-loaded DCs. In contrast, $CD4^+/CD25^{int}$ cells produced a strong proliferative response against tetanus toxoid, and a significant, albeit weaker, response, against RCC RNA-encoded antigens. No proliferative response against RE RNA- or PBMC RNA-transfected DCs (latter not shown) was observed. $CD4^+/CD25^{high}$ Tregs exhibited profound immunosuppressive activity in vitro, as evidenced by inhibition of allogeneic DC-stimulated mixed-lymphocyte reaction (MLR) cultures. The addition of increasing numbers of $CD4^+/CD25^{high}$ cells (1:5 responder cells; 1:1 responder cells) to MLRs led to a dose-dependent inhibition of responder T cell proliferation while $CD4^+/CD25^{high}$ T cells did not proliferate significantly upon stimulation with DCs (DC+Treg). Tregs demonstrated strong cell surface expression of glucocorticoid-induced TNF receptor family gene (GITR) as well as intracellular CTL-associated antigen-4 (CTLA-4) and forkhead box P3 transcriptional regulator (FoxP3) (Figure 1C). Stimulation of $CD4^+/CD25^{high}$ T cells using anti-CD3/CD28 antibodies resulted in enhanced expression of GITR, CTLA-4, and FoxP3 while $CD4^+$ T cells with negative or intermediate levels of CD25 exhibited significantly lower levels of these markers after nonspecific stimulation.

Since CD25 is not an optimal marker to enumerate Tregs in human subjects, as it is upregulated upon T cell activation, the number of *FoxP3* transcripts was determined in various T cell populations using quantitative real-time PCR. FoxP3 is the most specific Treg marker currently available while other molecules expressed by Tregs (i.e., CD45RB, CD38, and CD62L) previously failed to demonstrate specificity for detecting Tregs with immunosuppressive activity (15, 16). To determine the specificity of *FoxP3* for $CD4^+/CD25^+$ Tregs, $CD3^+$, $CD8^+$, $CD4^+$, $CD4^+/CD25^-$, and $CD4^+/CD25^+$ T cells were isolated from the PBMCs of healthy volunteers and from RCC patients by magnetic bead separation, and copy numbers of *FoxP3* mRNA were analyzed. Consistent with other reports (7, 17), high expression of FoxP3 protein (Figure 1C) and message (Figure 1D) were observed in $CD4^+/CD25^+$ T cells while $CD4^+/CD25^-$ and all other T cell subsets exhibited only low or background levels of *FoxP3* mRNA (Figure 1D, left panel). When corrected for cell population frequencies, $CD4^+/CD25^+$ T cells contributed 64% of *FoxP3* transcripts in the PBMC pool of healthy volunteers (84% in RCC patients) while $CD4^+/CD25^-$ cells accounted for 25% (14% in RCC patients). Less than 10%

**Table 1**
Patient characteristics and treatment assignments

| Subject[A] | Age (yr) | Sex | KPS (%) | Diagnosis | Metastases[B] | Treatments[C] | DAB dose[D] (μg) | No. of Tregs (% CD4+) | Treg depletion (%) | ELISPOT[E] CD8+ | ELISPOT[E] CD4+ | Diptheria titer | Time intervals (mo)[F] Dx | Nx | FU | Status |
|---|---|---|---|---|---|---|---|---|---|---|---|---|---|---|---|---|
| 01-RCC-DAB | 58 | M | 80 | RCC | LN/BN | Nx/MR | 2412 | 4.6 | 74 | 16.2 | 7.6 | 1:6561 | 36 | 36 | 24 | AWD |
| 02-RCC-DAB | 54 | M | 90 | RCC | BN | Nx/MR/Cyt/Ch/XRT | 1494 | 2.5 | 72 | 12.5 | 6.3 | 1:243 | 39 | 39 | 21 | AWD |
| 03-RCC-DAB | 69 | F | 90 | RCC | PN | Nx/MR | 1590 | 3.7 | 68 | 5.4 | 2.2 | Neg | 3 | 2 | 1 | DOD |
| 04-RCC-DAB | 60 | M | 90 | RCC | PN | Nx/Cyt/Ch/MR | 1906 | 3.8 | 76 | 7.4 | 9.7 | Neg | 170 | 204 | 5 | AWD |
| 05-RCC-DAB | 57 | M | 100 | RCC | ST/PN | Nx/MR | 1566 | 2.8 | 57 | 7.8 | 31.0 | N/D | 8 | 155 | 5 | AWD |
| 06-RCC-DAB | 61 | M | 90 | RCC | BN | Nx/XRT/Cyt/MR | 1301 | 4.2 | 26 | 8.0 | 6.8 | Neg | 14 | 26 | 6 | AWD |
| 07-OVA-DAB[G] | 56 | F | 90 | OVA | ST | TAH/Ch/MR/Cyt | 900 | 3.7 | 35 | 7.8 | 4.5 | 1:19683 | 35 | NA | 16 | AWD |
| 08-RCC | 60 | M | 70 | RCC | LN/BN | Nx/MR/Cyt | NA | 2.7 | NA | 0 | 1.0 | ND | 10 | 10 | 8 | DOD |
| 09-RCC | 61 | M | 75 | RCC | PN | Nx/MR | NA | 3.2 | NA | 5.1 | 2.0 | N/D | 5 | 5 | 3 | DOD |
| 10-RCC | 67 | M | 85 | RCC | PN/ST | Nx/Cyt/MR | NA | 3.0 | NA | 3.2 | 4.5 | ND | 16 | 16 | 11 | AWD |
| 11-RCC | 67 | M | 95 | RCC | PN | Nx/Cyt/MR | NA | 4.4 | NA | 2.1 | 2.0 | ND | 8 | 9 | 9 | AWD |

Vaccine, tumor RNA-transfected DC. [A]In subject identification numbers, DAB indicates pretreatment with $DAB_{389}$IL-2 4 days prior to DC vaccination, RCC indicates metastatic RCC, and OVA indicates metastatic ovarian carcinoma. [B]At time of study entry. [C]Prior to vaccination. [D]18 μg/kg. [E]Fold increase after vaccination. [F]Dx, time between first diagnosis of metastatic disease and first DC vaccination; Nx, time between nephrectomy and first DC vaccination; FU, time interval between last vaccination and last clinical/radiological follow-up. [G]Subject with ovarian carcinoma, not included in statistical analysis. AWD, alive with disease; BN, bony; Ch, chemotherapy (5-fluorouracil), Cyt, cytokines; DOD, dead of disease; KPS, Karnofsky performance status; MR, metastatic tumor resection; ND, not determined; Neg, negative; Nx, nephrectomy; PN, pulmonary nodule; ST, soft tissue; TAH, total abdominal hysterectomy; XRT, radiation therapy.

of *FoxP3* transcripts were expressed by $CD8^+$ T cells and $CD3^-$ cells (B cells, monocytes/macrophages, and NK cells; data not shown). When assayed by FACS, $CD4^+/CD25^{high}/FoxP3^+$ Treg frequencies detected in the peripheral blood of metastatic RCC patients after tumor nephrectomy ($n$ = 10) ranged from 2.5% to 4.6% and were significantly elevated (2.1 ± 1.2-fold increase) when compared with healthy volunteer controls ($n$ = 10). Accordingly, there was a statistically significant increase in the number of *FoxP3* transcripts that could be amplified from isolated $CD4^+$ T cells of RCC patients when compared with those of healthy volunteers ($P$ = 0.009) (Figure 1D, right panel).

In summary, we show that $CD4^+/CD25^{high}$ T cells isolated from the PBMCs of RCC patients exhibited suppressive activity while $CD4^+$ cells with negative or intermediate CD25 levels represented either naive/resting or memory/effector T cells. Therefore, in clinical settings, it will be important to identify suitable reagents that allow selective elimination of $CD25^{high}$ Tregs while sparing other cells expressing low or intermediate levels of CD25. Consistent with other reports (7, 18), higher Treg frequencies were measured in the peripheral blood of metastatic RCC patients when compared with healthy donor controls.

*Selective elimination of Tregs in vitro.* Human malignant cells overexpressing CD25 can be inactivated or eliminated using the recombinant IL-2 diphtheria toxin conjugate, denileukin difititox ($DAB_{389}$IL-2) (19). In order to determine whether $DAB_{389}$IL-2 could serve as a suitable reagent to achieve Treg depletion under clinically relevant conditions, we analyzed Treg susceptibility to $DAB_{389}$IL-2 in 3-(4,5-dimethylthiazol-2-yl)-2,5-diphenyl tetrazolium bromide salt (MTT) assays. In these experiments, we chose conditions that resembled the pharmacokinetics of a single intravenous dose of $DAB_{389}$IL-2 (18 μg/kg) corresponding to 5 nM peak plasma concentrations. In previous clinical trials, this dose level demonstrated optimal clinical efficacy and acceptable toxicity profiles (20). Given a plasma half-life of approximately 60 minutes and a dissociation constant of 1 pM for $DAB_{389}$IL-2 and the high-affinity IL-2 receptor, $DAB_{389}$IL-2 plasma levels were projected to reach suboptimal concentrations after 6 hours. Therefore, in the experiments shown in Figure 2A, the viability of isolated $CD4^+/CD25^{high}$ T cells was analyzed after a 6-hour exposure to increasing concentrations of $DAB_{389}$IL-2 (range 0.05–5.0 nM) in vitro over 48 hours. For $CD4^+/CD25^{high}$ Tregs, a significant reduction in cell viability was observed 24 hours after exposure to $DAB_{389}$IL-2. Efficient killing of $CD4^+/CD25^{high}$ cells was noted at 0.5 nM concentrations after 48 hours while complete depletion was achieved at a 5 nM concentration. In contrast, exposure of $CD4^+/CD25^{neg}$ and $CD4^+/CD25^{int}$ cells to $DAB_{389}$IL-2 did not result in significant cell death except when these cells were exposed to $DAB_{389}$IL-2 concentrations higher than 10 nM (latter not shown). In another set of experiments, $DAB_{389}$IL-2 used at a 5 nM concentration resulted in specific killing of Tregs but not of other bystander cells in vitro. As shown in Figure 2A, there were no significant differences in PBMC viability over time when $DAB_{389}$IL-2 (5 nM) was added to the culture. In contrast, when PBMCs and Tregs were mixed (1:1 ratio), cell viability was reduced by more than 60% after 48 hours, suggesting selective, diphtheria toxin–mediated Treg killing without bystander toxicity. In order to corroborate these findings, 7-amino-actinomycin D (7-AAD) staining was performed on $CD4^+$ T cell populations with increasing densities of CD25 (Figure 2B). Consistent with the experiments shown in Figure 2A, optimal killing of $CD4^+/CD25^{high}$ Tregs was achieved using 5-nM $DAB_{389}$IL-2 concentrations while $DAB_{389}$IL-2 exposure to other $CD4^+$ T cells with lower or no CD25 expression revealed only background levels of 7-AAD staining.

Next, the impact of $DAB_{389}$IL-2 on freshly activated lymphocytes was analyzed after stimulation with allogeneic DCs in MLR cultures. $DAB_{389}$IL-2–mediated Treg depletion prior to initiation of MLR culture resulted in a 2-fold increase in proliferation of responder cells (PBMC±DAB). Conversely, the addition of isolated Tregs (DC+Treg) resulted in an

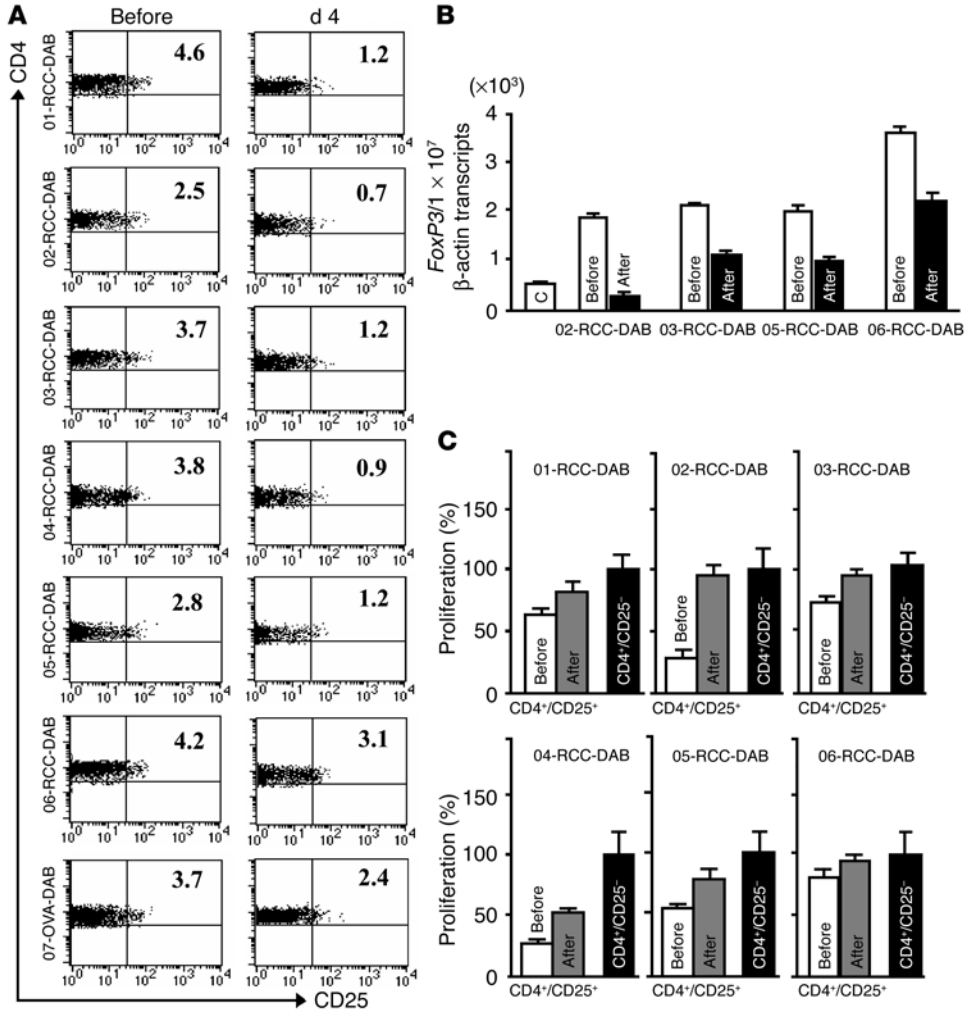


**Figure 3**
Depletion of Tregs in study subjects. (**A**) $CD4^+$ T cells isolated from all $DAB_{389}$IL-2–treated study patients were analyzed by flow cytometry for expression of CD25 prior to and 4 days after intravenous administration; percentages of $CD4^+/CD25^{high}$ T cells are shown. (**B**) Reduction of *FoxP3* mRNA copy numbers before and after $DAB_{389}$IL-2 treatment was determined by $CD4^+$ T cells derived from 4 study subjects, as described in the legend to Figure 1D. The average *FoxP3* mRNA copy number averaged from 5 healthy volunteers was used as control (C). (**C**) Functional analysis of Tregs isolated from study subjects prior to and after $DAB_{386}$IL-2 administration. $CD4^+/CD25^+$ and $CD4^+/CD25^-$ T cell subsets were isolated from PBMC samples by magnetic bead separation, and Treg-mediated inhibition of activated $CD4^+/CD25^-$ indicator T cells was measured according to a protocol described previously (28).

approximately 80% reduction in T cell proliferation (1:1 Treg/responder ratio) (Figure 2C). Preincubation of Tregs with 5-nM $DAB_{389}$IL-2 (DC+Treg+DAB) significantly abrogated their inhibitory effect when added to MLR; however, responder cells did not proliferate as vigorously as in the absence of Tregs, suggesting potential contact inhibition by Tregs, as reported previously (21). Importantly, the addition of $DAB_{389}$IL-2 two days after initiation of MLR (DC+DAB) completely abrogated the proliferation of responder cells, suggesting that $DAB_{389}$IL-2 eliminated not only Tregs but also freshly activated naive T cells that acquired CD25 expression.

These experiments suggest that $DAB_{389}$IL-2 is a suitable reagent for selectively eliminating Tregs in vitro without affecting other lymphocytes, including naive and memory T cells with negative or intermediate expression levels of CD25, respectively. Our data further indicate that in a vaccination setting, $DAB_{389}$IL-2 should only be applied prior to immunization but not during the vaccination phase, since activated effector T cells appear susceptible to $DAB_{389}$IL-2–mediated toxicity.

*Enhancement of T cell responses after Treg depletion in vitro.* To provide evidence that $DAB_{389}$IL-2–mediated Treg depletion is capable of augmenting antigen-specific T cell responses in vitro, CTLs were stimulated from PBMCs that were pretreated with or without $DAB_{389}$IL-2 (5 nM) (Figure 2D). PBMCs were stimulated twice with autologous DCs transfected with human telomerase reverse transcriptase (*hTERT*) and melanocyte antigen recognized by T cells 1 (*MART-1*) mRNA. In addition, DCs pulsed with an HLA-A0201–restricted MART-1 peptide were used as stimulators. RNA-transfected DCs were not only used as stimulators but also served as specific or control targets, as described previously (2, 22–24). The ability of the stimulated, antigen-specific CTLs to recognize their cognate but not control target cells was analyzed in standard cytotoxicity assays. As shown in Figure 2D, CTLs stimulated from Treg-depleted PBMCs exhibited significantly higher lytic activity against antigens encoded by *hTERT* or *MART-1* mRNA than CTLs stimulated from nondepleted PBMCs. In contrast, only modest, statistically insignificant improvement of antigen-specific killing was observed when MART-1 peptide–pulsed DCs were used as stimulators.

These data suggest that depletion of Tregs from human PBMCs enhances the stimulation of antigen-specific CTLs in vitro. It appears that among other factors, the impact of this strategy is influenced by the strength of the antigenic signal (25), as evidenced by the fact that T cell responses against mRNA-encoded self antigens was significantly enhanced. In contrast, the Treg-depletion strategy was less effective in improving CTL responses when DCs presenting high densities of peptide-MHC complexes (peptide pulsing) were used for stimulation.

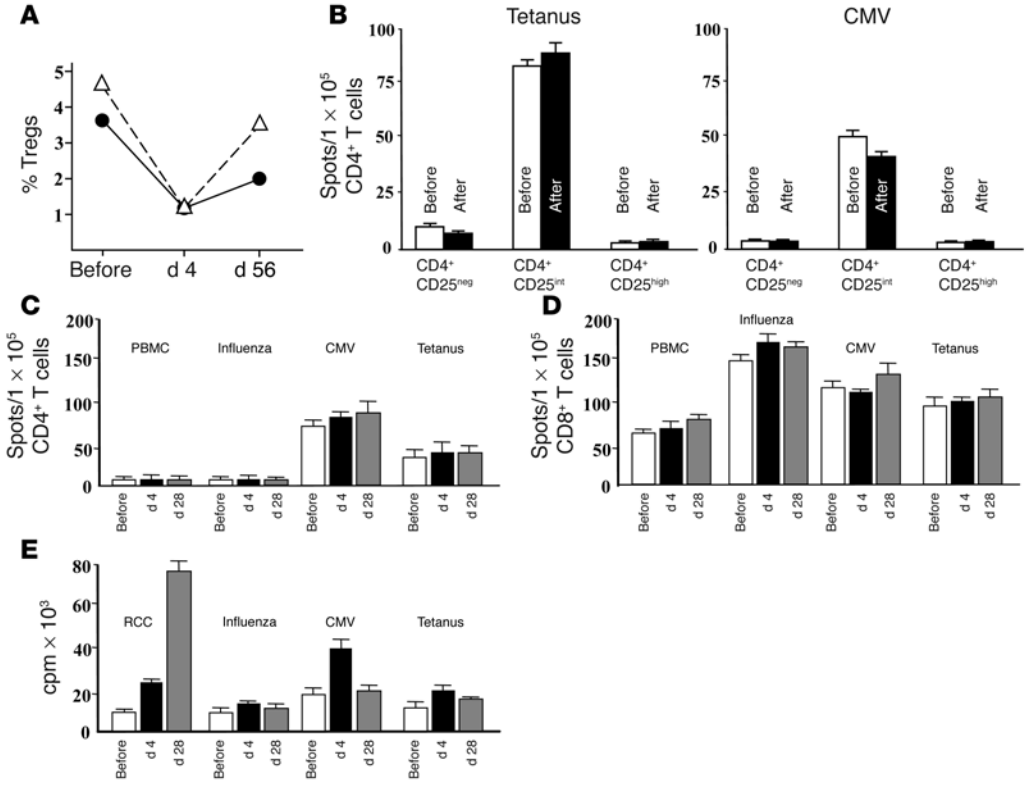


**Figure 4**
Specificity of Treg depletion. (**A**) Calculated CD4+/CD25$^{high}$ Treg frequencies in 2 study subjects (01-RCC-DAB; 03-RCC-DAB) prior to, 4 days after, and 2 weeks after final vaccination (study week 8; d 56). (**B**) IFN-γ ELISPOT were performed on sorted CD4+CD25$^{neg}$, CD4+CD25$^{int}$, and CD4+CD25$^{high}$ T cell subsets using tetanus toxoid and CMV lysate–pulsed DCs as stimulators. (**C**–**E**) In separate experiments, IFN-γ ELISPOT and antigen-specific proliferation analyses were performed on T cells isolated prior to vaccination and 4 and 28 days after $DAB_{389}$IL-2 treatment (results from patient RCC-01-DAB). For ELISPOT assays, $1 \times 10^5$ purified CD4+ T cells (**C**) or $1 \times 10^5$ purified CD8+ T cells (**D**) were stimulated with $1 \times 10^4$ DCs that were transfected with *fluM1* mRNA, autologous PBMC RNA, CMV lysate (20 μg/ml), or tetanus toxoid (0.5 μg/ml). After 18 hours, visible spots were enumerated using an automated ELISPOT reader. The same stimulators and RCC RNA-transfected DCs were used in proliferation assays (**E**). For proliferation assays, isolated CD3+ T cells were used as responders. Assays were performed at a stimulator/responder ratio of 1:10. After 4 days, cells were pulsed with 1 μCi of $^3$H-thymidine, and incorporated radioactivity was determined after 16 hours by liquid scintillation counting.

*Depletion of Tregs in vivo*. Having shown that Treg elimination is capable of enhancing T cell responses in vitro, a clinical study was initiated to test the Treg-depletion concept in a human vaccination setting. A total of 11 patients, including 10 with metastatic RCC and 1 with disseminated ovarian carcinoma (OVA), were treated in a study approved by the Duke University Institutional Review Board and the FDA. Seven subjects received a single intravenous dose of $DAB_{389}$IL-2 (18 μg/kg) 4 days prior to vaccination with tumor RNA-transfected DCs while a second cohort of 4 subjects was treated with the vaccine alone (Table 1). Outside the study, PBMCs were obtained from 1 additional RCC subject who received a single dose of $DAB_{389}$IL-2 (18 μg/kg) but no vaccine. Consistent with reports of others, $DAB_{389}$IL-2–related toxicities included grade I constitutional symptoms such as low-grade fever and malaise ($n$ = 4), grade I elevation of serum rheumatoid factor ($n$ = 1), and transient grade II serum alanine aminotransferase (ALT) elevations ($n$ = 1) (11). RNA-transfected DC injections were well tolerated without any major clinical toxicities or serologic/immunologic evidence of autoimmunity (2, 26).

In order to quantify the presence of CD4+/CD25$^{neg}$, CD4+/CD25$^{int}$, and CD4+/CD25$^{high}$ T cells in PBMC samples collected prior to and after $DAB_{389}$IL-2 treatment, flow cytometry was performed on patient-derived PBMC samples (Figure 3A). Gates were set on CD4+/CD25$^{high}$ T cells that constitutively expressed FoxP3 protein, as shown in Figure 1C. In all 7 subjects analyzed, $DAB_{389}$IL-2 administration resulted in significant reduction (range 26% to 76%) of CD4+/CD25$^{high}$ Tregs 4 days following intravenous infusion. Additional evidence that Tregs were depleted and that CD25$^{neg/int}$ T cell subsets were unaffected was provided by the observation that the number of total CD25$^{pos}$ cells measured in each patient after $DAB_{389}$IL-2 administration decreased correspondingly with the number of depleted CD4+/CD25$^{high}$ Tregs (data not shown). Moreover, as shown in 4 RCC patients from whom sufficient cells were available for analysis (02-RCC-DAB, 03-RCC-DAB, 05-RCC-DAB, and 06-RCC-DAB), $DAB_{389}$IL-2 treatment resulted in a significant reduction of *FoxP3* transcripts after $DAB_{389}$IL-2 treatment, as determined by quantitative real-time PCR (Figure 3B). In these subjects, *FoxP3* mRNA copy numbers (normalized to β-*actin* transcripts) were reduced by approximately 30% to 80% within purified blood CD4+ cells 4 days after $DAB_{389}$IL-2 administration. Finally, CD4+/CD25+ T cells isolated prior to but not 4 days after $DAB_{386}$IL-2 treatment consistently inhibited anti-CD3/CD28-mediated activation of CD4+/CD25− indicator T cells in all RCC subjects analyzed (Figure 3C), suggesting abrogation of Treg-mediated immunosuppressive activity in vivo. Notably, $DAB_{389}$IL-2–mediated Treg elimination was transient, since approximately 75% of Tregs were restored within 2 months in the patients' peripheral T cell pool (Figure 4A).

In 5 of 6 evaluable $DAB_{389}$IL-2–treated subjects, minor reductions (averaging 10%) in absolute neutrophil counts were observed while 1 subject exhibited a decrease of 20%. Accordingly, among these 5 with only minor absolute neutrophil count reductions, there were no significant changes in the relative number of CD3+, CD4+, and CD8+ T cells, B cells, monocytes/macrophages (CD14), and NK cells after treatment. In order to address the concern that

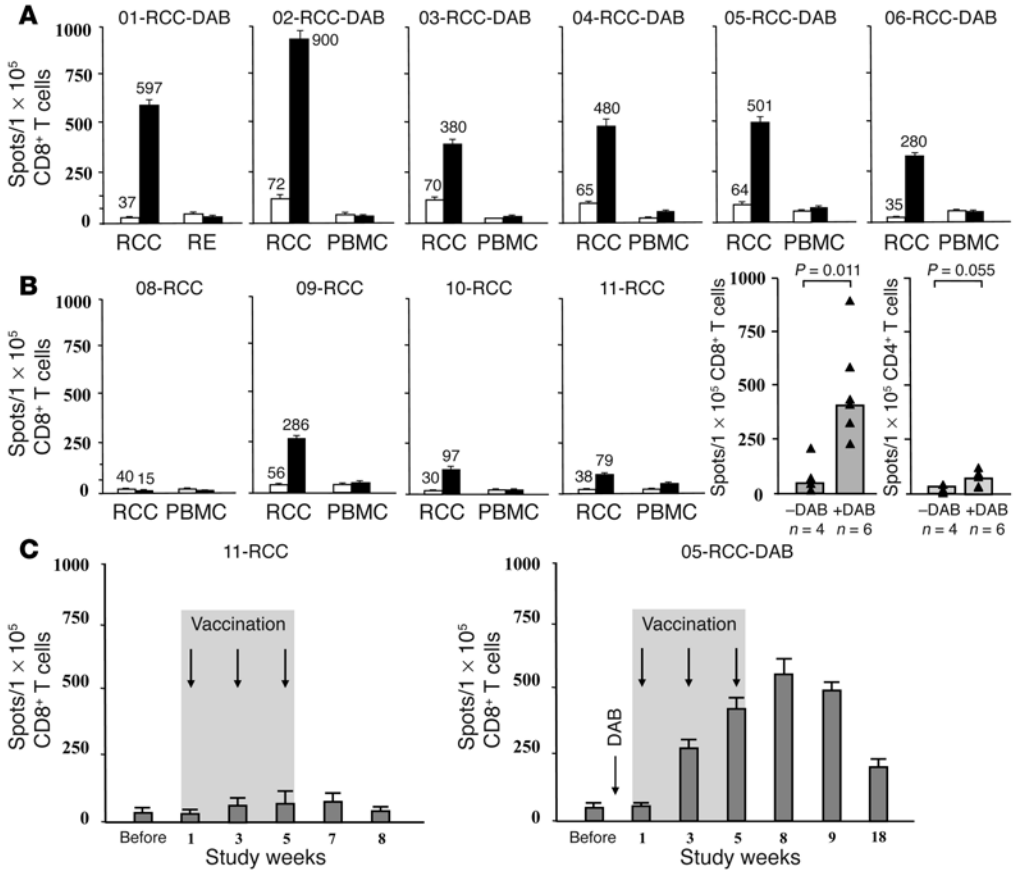


**Figure 5**
In vivo induction of tumor-specific T cell responses. (**A**) $CD8^+$ and $CD4^+$ T cells were isolated from prevaccination (white bars) and postvaccination (black bars) PBMCs of patients treated with $DAB_{389}$IL-2 and RCC RNA-transfected DCs. For vaccination, 3 doses of $1 \times 10^7$ cells injected intradermally every other week were administered. Isolated $CD8^+$ and $CD4^+$ T cells were stimulated for 18 hours with tumor RNA-transfected DCs, RE, or PBMC RNA-transfected DCs (controls). Visible spots were enumerated, and antigen-specific T cell frequencies were expressed as the number of spots forming cells per $1 \times 10^5$ T cells. (**B**) Left panels: stimulation of tumor-specific $CD8^+$ in 4 subjects treated with tumor RNA-transfected DCs alone. Right panels: summary of $CD8^+$ and $CD4^+$ T cell responses from 4 subjects receiving immunization alone (–DAB) or from 7 patients treated with combined therapy (+DAB). Bars indicate the median value of all subjects analyzed. Filled triangles represent T cell frequencies of individual patients. (**C**) Temporal evolution of tumor-specific $CD8^+$ T cells after vaccination. IFN-γ ELISPOT analyses on sorted $CD8^+$ T cells were performed as described in **A**. Frequencies of tumor-specific T cells prior to, during, and after immunization are presented for 2 patients who received 3 vaccinations with tumor mRNA-transfected DCs alone (11-RCC) or were treated with $DAB_{389}$IL-2 (01-RCC-DAB) followed by vaccination.

istration (DAB) and 2 weeks after 3 vaccination cycles. Over the entire treatment cycle, no differences were observed in the absolute number of T cells with specificity against PBMC RNA-transfected DCs, *influenza virus matrix protein 1* (*fluM1*) mRNA-transfected DCs, CMV lysate–loaded DCs, or tetanus toxoid–loaded DCs. Furthermore, antigen-specific proliferation assays (Figure 4E) revealed strong reactivities against renal tumor antigens and unchanged reactivities against the prototype recall antigens fluM1/tetanus toxoid.

Cumulatively, the experiments shown in Figures 3 and 4 demonstrate that administration of a single dose of $DAB_{389}$IL-2 resulted in significantly reduced numbers of Tregs in the peripheral blood of RCC patients (Figure 3, A and B) and in significant abrogation of Treg-mediated suppressive activity (Figure 3C). Our data further suggest that $DAB_{389}$IL-2–mediated toxicities against other hematopoietic cells expressing CD25 are unlikely and that lymphopenia-induced T cell proliferation (27) may not represent a significant issue in a vaccination setting.

*In vivo stimulation of tumor-specific T cell responses.* In order to determine whether $DAB_{389}$IL-2–mediated Treg depletion is capable of augmenting vaccine-induced $CD8^+$ and $CD4^+$ T cell responses in cancer patients, IFN-γ ELISPOT analyses were performed to determine the frequencies of vaccine-induced, tumor-specific T cells from PBMC samples collected before and 2 weeks after the third vaccination. $CD8^+$ and $CD4^+$ T cells were isolated from pre- and post-vaccination PBMCs and cultured overnight with tumor RNA-transfected DC targets. As controls, autologous PBMC RNA and/or autologous benign RE-derived RNA-transfected DCs were used for short-term antigenic stimulation. As shown in Figure 5, A and B, only background levels of RE- or PBMC-specific T cells were observed prior to or after vaccination. Also, tumor-specific T cell responses did not significantly increase in independently evaluated subjects after treatment with $DAB_{389}$IL-2 alone over a period of 28 days (data not shown). In contrast, all

$DAB_{389}$IL-2–mediated Treg depletion may induce toxicity within the memory T cell pool ($CD4^+/CD25^{int}$), a series of experiments was performed analyzing $CD4^+/CD25^{int}$ T cell function prior to and 4 days after $DAB_{389}$IL-2 administration. First, IFN-γ ELISPOT analyses were performed on sorted $CD4^+/CD25^{neg}$, $CD4^+/CD25^{int}$, and $CD4^+/CD25^{high}$ T cell subsets using tetanus toxoid or CMV lysate–pulsed DCs as stimulators. As shown in Figure 4B, only $CD4^+/CD25^{int}$ memory T cells were capable of stimulating T cell responses against tetanus or CMV antigens while naive ($CD4^+/CD25^{neg}$) and $CD4^+/CD25^{high}$ T cells failed to stimulate T cell responses of a significant magnitude. In a second set of experiments, the frequency of IFN-γ secreting T cells was analyzed using $CD4^+$ (Figure 4C) and $CD8^+$ responder T cells isolated from human PBMCs (Figure 4D) prior to and 4 days after $DAB_{389}$IL-2 admin-

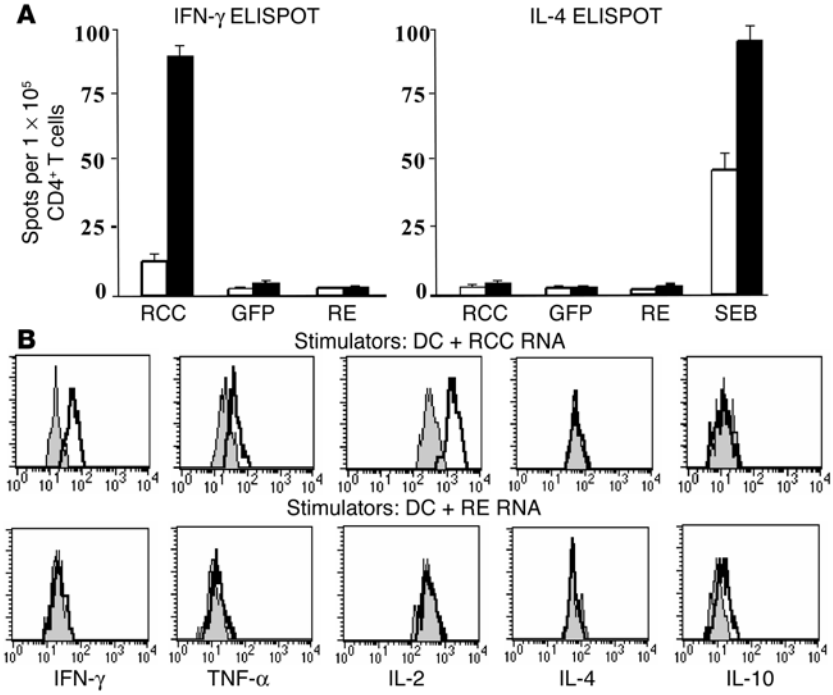


**Figure 6**
In vivo induction and cytokine profile of RCC-specific CD4+ T cell responses. (**A**) CD4+ T cells were isolated from pre- (white bars) and post-vaccination (black bars) PBMC samples of 3 study subjects (representative data from patient RCC-01-DAB are shown) who received $DAB_{389}$IL-2 (18 μg/kg) followed by vaccination with RCC RNA-transfected DCs (2 cycles of $1 \times 10^7$ cells per treatment). Cells were stimulated for 18 hours with autologous PBMC RNA-, RE RNA-, or RCC RNA-transfected DCs. IFN-γ (left panel) or IL-4–expressing T cells (right panel) were enumerated using an automated ELISPOT reader, and antigen-specific T cell frequencies were expressed as the number of spot-forming cells per $1 \times 10^5$ CD4+ T cells. Staphylococcal enterotoxin B (SEB) at a concentration of 10 μg/ml was used as a positive control in the IL-4 ELISPOT assays (right panel). (**B**) The cytokine expression profile of CD4+ T cells prior to (gray) and after (white) vaccination was measured after overnight (18 hours) stimulation with RCC (DC+RCC) or RE RNA-transfected DCs (DC+RE) using human Th1/Th2 cytometric bead arrays. Culture supernatants were used to determine expression of the Th-1 cytokines IFN-γ, TNF-α, and IL-2 as well as the Th-2 type cytokines IL-4 and IL-10.

but 1 (08-RCC) patient immunized with tumor RNA-transfected DCs exhibited significant increases in tumor-specific CD8+ and CD4+ T cell frequencies after vaccination (Figure 5B and Table 1). A 2.7-fold median increase (range 0 to 5.1) of tumor-specific CD8+ T cells and a 2.0-fold median increase in tumor-specific CD4+ T cells (range 1.0 to 4.5) was observed in the subjects receiving vaccination alone (Table 1). Although there was significant patient-to-patient variability in the magnitude of T cell responses measured in each patient, vaccination after Treg depletion stimulated significantly higher numbers of tumor-specific CD8+ T cells in RCC patients receiving $DAB_{389}$IL-2 plus RCC RNA-transfected DCs, when compared with RCC patients receiving vaccination alone ($P = 0.011$). Moreover, there was a trend toward improved CD4+ T cell responses ($P = 0.055$) in RCC patients treated with combined therapy (Figure 5B). A 7.9-fold median increase in the number of tumor-specific CD8+ T cells (range 5.4 to 16.2) and a 7.2-fold median increase in CD4+ T cells (range 2.2 to 31.0) was detected in the 6 RCC patients receiving $DAB_{389}$IL-2 plus vaccination with RCC RNA-transfected DCs. The absolute CD8+ T cell frequencies achieved with combined therapy were remarkably high with up to 0.90% of CD8+ T cells exhibiting tumor specificity after 3 vaccinations. In order to evaluate the temporal evolution of the T cell response stimulated by vaccination with or without $DAB_{386}$IL-2 therapy, longitudinal monitoring of vaccine-induced CD8+ T cell responses was performed using IFN-γ ELISPOT in 2 subjects from whom sufficient numbers of cells were available for analysis (11-RCC and 05-RCC-DAB). $DAB_{389}$IL-2–mediated Treg depletion followed by vaccination resulted in a significantly enhanced and also prolonged CD8+ T cell response when compared with the subject receiving vaccination alone. As demonstrated recently (26), the vaccine-induced and tumor-specific CTL response surged over the entire treatment course and peaked approximately 2 weeks after the third and final dose (Figure 5C).

In additional experiments, the cytokine secretion profiles by vaccine-induced and tumor-specific CD4+ T cells were analyzed after combined $DAB_{389}$IL-2 and active immunotherapy (Figure 6, A and B). PBMCs were collected from 3 study subjects at baseline and 2 weeks after the final vaccination, and CD4+ T cells were isolated by magnetic bead sorting. CD4+ T cells were restimulated for 18 hours with renal tumor RNA-transfected DCs and analyzed for IFN-γ and IL-4 secretion using ELISPOT analysis. As control targets, *GFP* mRNA-, RE RNA-transfected DCs, and staphylococcal enterotoxin B (SEB) were used. As shown in Figure 6A, vaccination after Treg depletion resulted in significant stimulation of IFN-γ but not IL-4–secreting renal tumor–specific CD4+ T cells while no stimulation against GFP or RE-expressing targets was noted. In addition, human Th1/Th2 flow cytometry–based bead arrays (Figure 6B) confirmed secretion of the Th-1 type cytokines IL-2 (increase from 680 to 1270 pg/ml), IFN-γ (160 to 270 pg/ml), and TNF-α (34 to 59 pg/ml) but not Th-2 type cytokines (IL-10 and IL-4) by vaccine-induced CD4+ T cells 18 hours after stimulation with RCC RNA-transfected DCs. This effect was not seen when RE RNA-transfected DCs were used as stimulators. These data further suggest that the vaccine-induced tumor-specific T cell response is directed against tumor-associated antigens but not gene products expressed by normal RE.

In conclusion, we show that Treg depletion using the diphtheria fusion protein $DAB_{389}$IL-2 is capable of enhancing a vaccine-induced T cell response in patients with advanced RCC. Although only a limited number of patients were studied in this clinical trial, an up to 16-fold increase in tumor-specific CTL frequencies could be measured in subjects receiving combined treatment when compared with individuals receiving vaccination alone. The vaccine-induced T cell frequencies achieved without Treg depletion were similar to those observed in a prior study in which immature tumor RNA-transfected DCs were used for vaccination (1).

## Discussion

The objective of this study was to enhance the immunostimulatory efficacy of RNA-transfected DC vaccines by selectively eliminating $CD4^+/CD25^{high}$ Tregs in metastatic RCC patients. For Treg depletion, we used the recombinant fusion protein denileukin diftitox ($DAB_{389}$IL-2) (20) in a human vaccination setting. We show that human $CD4^+CD25^{high}$ Tregs can be eliminated using a single dose of $DAB_{389}$IL-2 without apparent bystander toxicity and without having an impact on the function of other cells expressing CD25. However, $DAB_{389}$IL-2 also abrogated DC-mediated activation of T cells in vitro, suggesting that the applicability of this reagent should be restricted to a prevaccination setting (Figure 2C). These preclinical results provided important information regarding the design of our clinical study, in which $DAB_{389}$IL-2 was administered to RCC patients 4 days prior to DC-based vaccination. This time interval was chosen since, unlike antibodies, $DAB_{389}$IL-2 is characterized by a short duration of action, with a half-life of approximately 60 minutes, thereby minimizing the possibility of interfering with the ongoing vaccine-induced T cell response.

In this study, $DAB_{389}$IL-2 profoundly reduced the number of Tregs present in the peripheral blood of RCC patients, reduced levels of peripheral blood–derived *FoxP3* transcripts, and abrogated Treg-mediated immunosuppressive activity in vivo. Moreover, significantly higher frequencies of tumor-specific $CD8^+$ T cells could be measured in patients treated with combined $DAB_{389}$IL-2 and vaccination when compared with subjects receiving the vaccine alone. Also, there was a trend toward an improved $CD4^+$ T cell response after combined therapy. Cumulatively, these data provide several independent lines of evidence that Tregs were depleted in the peripheral blood of RCC patients by using a single dose of the fusion protein $DAB_{389}$IL-2.

The T cell frequencies achieved after Treg depletion and 3 vaccination cycles were remarkably high with up to 0.90% of all $CD8^+$ T cells demonstrating tumor specificity. No clear correlation between the efficacy of Treg depletion and the magnitude of the vaccine-induced T cell response was observed. Also, serum diphtheria titers did not appear to have an impact on vaccine efficacy (11). The present study further suggests that the degree of Treg depletion achieved using a single dose of 18 μg/kg may be quite variable and that Treg depletion was transient, with most cells returning after 2 months. However, it should be pointed out that the exact enumeration of Tregs in a vaccination setting is complicated by the fact that $CD4^+$ T cells with negative or intermediate expression levels of CD25 may upregulate expression of CD25 in response to antigenic stimulation, thereby biasing results towards increased detection of Tregs. Our preclinical studies also suggest that the Treg strategy may be geared toward the improvement of T cell responses against relatively weak self antigens such as hTERT or MART-1 antigens but not against immunodominant peptide-derived antigens (Figure 2D). Accordingly, other studies have recently shown that Tregs effectively suppress the physiologic activation of autoreactive T cells associated with low strength of the antigenic signal while T cells activated with high antigenic signal strength were refractory to this mechanism of suppression (25). Although in this study, the concept of Treg elimination has been employed in context with RNA-transfected DC-based vaccination, this strategy could potentially be applied to many immune-based approaches of active and passive immunotherapy as well as to classical adjuvants. The information gained from this study will serve as a baseline for further clinical investigation to better define the full potential of this strategy in ultimately achieving antitumor immunity with clinical impact. For such studies it will be critical to collect precise information on Treg depletion and vaccine-induced T cell response and, ultimately, address the clinical efficacy of such strategy in cancer patients.

## Methods

*Clinical trial design and patient eligibility*. Treatment of patients was performed following written informed consent as part of a protocol approved by an Institutional Review Board and the FDA. Patients with histologically confirmed metastatic RCC were eligible for this study. One patient with disseminated OVA was included and treated on a compassionate basis. All patients were required to have adequate hepatic, renal, and neurological function, a life expectancy of more than 6 months, and a Karnofsky performance status of greater than or equal to 70%. Patients had to have recovered from all toxicities related to any prior therapy and not received any chemotherapy, radiation therapy, or immunotherapy for at least 6 weeks prior to study entry. Excluded from the study were patients with CNS metastases, with a history of autoimmune disease, and with serious intercurrent chronic or acute illnesses. Patients on immunosuppressive agents were also excluded. Eligible subjects were randomized with equal probability to receive either a single dose of $DAB_{389}$IL-2 (18 μg/kg) followed by vaccination with tumor RNA-transfected DCs or vaccination alone. All subjects received 3 intradermal injections of tumor RNA-transfected DCs. The injections were given intradermally at biweekly intervals and consisted of $1 \times 10^7$ cells suspended in 200 μl 0.9% sodium chloride at each vaccination. Following treatment, subjects were evaluated for clinical toxicity and immunological and clinical responses. Due to regulatory restrictions and, in some subjects, limited access to tumor tissue, no tumor biopsies were performed.

*$DAB_{389}$IL-2 and vaccine preparation*. $DAB_{389}$IL-2 (ONTAK; Ligand Pharmaceuticals) was provided as a frozen, sterile solution formulated in citrate buffer in 2 ml single-use vials at a concentration of 150 μg/ml. After thawing, $DAB_{389}$IL-2 was diluted with sterile normal saline to a final concentration of 15 μg/ml and delivered by intravenous infusion over a 30-minute period. Patients were permitted to receive acetaminophen (600 mg) and antihistamines 30 to 60 minutes prior to infusion. For DC culture, a concentrated leukocyte fraction was harvested by leukapheresis. PBMCs were isolated from the leukapheresis product by density gradient centrifugation (Histopaque; Sigma-Aldrich). The semiadherent cell fraction was used for DC culture in serum-free X-VIVO 15 medium (Cambrex Corp.) supplemented with recombinant human IL-4 (500 U/ml) (R&D Systems) and recombinant human GM-CSF (rhGM-CSF) (800 U/ml) (Immunex Corp.). After 7 days, immature DCs were harvested and transfected with total RNA extracted from tumor tissues histologically classified as clear cell carcinoma. Control RNA used for immunological monitoring studies was isolated from autologous benign renal tissues (RE) or from PBMCs. Transfection of immature DCs was carried out by electroporation. DCs were washed in PBS and resuspended at a concentration of $4 \times 10^7$ cells/ml in ViaSpan (Barr Laboratories). Cells were then coincubated for 5 minutes with 5 μg RNA per $1 \times 10^6$ cells and electroporated in 0.4 cm cuvettes via exponential decay delivery at 300 V and 150 μF (Gene Pulser II; Bio-Rad). After electroporation, cells were resuspended in X-VIVO 15 medium and matured for 20 hours in the presence of 10 ng/ml TNF-α, 10 ng/ml IL-1β, 150 ng/ml IL-6 (R&D Systems), and 1 μg/ml prostaglandin $E_2$ ($PGE_2$) (Cayman Chemical Co.). Prior to administration, cells were characterized to ensure that they met the typical phenotype of fully mature DCs: $Lin^{neg}$, HLA class I and $II^{high}$, $CD86^{high}$, and $CD83^{high}$.

*Evaluation of immune status*. IFN-γ and IL-4 ELISPOT analyses were performed using PBMCs obtained prior to, during, and after vaccination. PBMCs were cultured overnight in complete RPMI 1640 medium. $CD4^+$ and $CD8^+$ T cells were isolated from PBMCs by negative depletion (Miltenyi Biotec). After blocking, $1 \times 10^5$ T cells and $1 \times 10^4$ RNA-transfected DCs were added to each well of 96-well nitrocellulose plates (Multiscreen-IP; Millipore) precoated with 2 μg/ml IFN-γ capture antibody (Pierce Biotechonology Inc.) or with IL-4 capture antibody (BD Biosciences — Pharmingen). Plates were incubated for 20 hours at 37°C, and biotinylated IFN-γ detection antibody (Pierce Biotechonology Inc.) or biotinylated IL-4 antibody (BD Biosciences — Pharmingen) was added to each well. Cells were then incubated for an additional 2 hours at room temperature, then with streptavidin-alkaline phosphatase (1 μg/ml; Sigma-Aldrich); plates were developed with substrate (KPL). After washing, spots were counted using an automated ELISPOT reader (Zeiss). CTL assays were performed by coculturing RNA-transfected DCs with autologous PBMCs. Cells were restimulated once, and IL-2 (20 units/ml) was added after 5 days and every other day thereafter. After 12 days of culture, effector cells were harvested. Target cells were labeled with 100 μCi of $Na_2[^{51}CrO_4]$ (PerkinElmer) in 200 μl of complete RPMI 1640 for 1 hour at 37°C in 5% $CO_2$, and $^{51}Cr$-labeled target cells were incubated in complete RPMI 1640 medium with effector cells for 5 hours at 37°C. Then 50 μl of supernatant was harvested, and release of $^{51}Cr$ was measured with a scintillation counter. For proliferation assays, purified $CD3^+$ T cells were seeded into round-bottomed microplates in the presence of mRNA-transfected DCs. T cells alone were used as the background control. After 4 days, 1 μCi of [*methyl*-$^3$H] thymidine (PerkinElmer) was added to each well for an additional 16 hours. Incorporation of thymidine was determined using a liquid scintillation counter. Cytotoxicity of $DAB_{389}$IL-2 was determined in MTT assays. After 6 hours incubation with varying concentrations of $DAB_{389}$IL-2, cells were seeded in 96-well plates at a density of $5 \times 10^3$ cells/well. After 48 hours of incubation, 20 μl MTT from a 5 mg/ml stock was added. After 4 hours, the formazan crystals were solubilized by adding 100 μl isopropanol/0.1 M hydrochloric acid. The absorbance of the formazan product was measured on an ELISA plate reader at 570 nm. Cytokine secretion by vaccine-induced $CD4^+$ T cells was measured using the human Th-1/Th-2 cytokine kit (Cytokine Bead Array; BD Biosciences — Pharmingen) according to the manufacturer's instructions. Isolated $CD4^+$ T cells were restimulated overnight with RNA-transfected DCs at a ratio of 10:1.

*FACS analysis*. Four-color FACS analyses were performed using the following antibodies: anti-CD4 FITC, anti-CD45RO, anti-CD45RA (CALTAG Laboratories), anti-CD25 PE (BD Biosciences — Pharmingen), and anti-GITR (R&D Systems) as well as isotypic controls (CALTAG Laboratories). Sorting of $CD4^+/CD25^{neg}$, $CD4^+/CD25^{int}$ and $CD4^+/CD25^{high}$ T cells was performed using a BD FACSAria cell sorter after antibody labeling. For intracellular detection of FoxP3, cells were permeabilized with 30 μg/ml digitonin for 45 minutes at 4°C. Subsequently, cells were stained with anti-FoxP3 antibody (Abcam), and R-phycoerythrin anti-goat IgG in the presence of 10 μg/ml digitonin for 30 minutes at 4°C. Following staining, cells were fixed and analyzed by FACS. For intracellular CTLA-4 detection, T cells were permeabilized, fixed, and stained with biotinylated anti-CD152 (BD Biosciences — Pharmingen) followed by APC-strepavidin (BD Biosciences — Pharmingen). A total of $1 \times 10^6$ cells were suspended in staining buffer (PBS with 1% FCS, 2 mM EDTA, and 0.1% sodium azide) and incubated for 20 minutes at 4°C with the antibody.

*Treg functional evaluation*. The suppressive activity of Tregs isolated from PBMCs of study subjects prior to and 4 days after $DAB_{386}$IL-2 administration was analyzed, as described previously (28). $CD4^+/CD25^+$ T cells were isolated from the PBMCs of study subjects using magnetic bead separation techniques. Cells were washed with PBS, resuspended in complete RPMI 1640 medium, and placed into 96-well round bottom plates precoated with anti-CD3/CD28 antibodies (0.4 μg/well) (CALTAG Laboratories). $CD4^+/CD25^-$ cells were plated at $2.0 \times 10^4$/well alone or in combination with $CD4^+/CD25^+$ cells in triplicate wells at a ratio of 1:2 ($CD4^+/CD25^-$:$CD4^+CD25^+$). On day 5, 1 μCi of $^3$H thymidine was added for the final 16 hours of the cultures. Cells were then harvested on glass fiber filters and assessed for uptake of radiolabeled thymidine.

*Detection of FoxP3 transcripts*. Details of real-time PCR–based quantification of β-*actin* transcripts were previously provided by Heiser et al. (2). *FoxP3* mRNA transcripts were quantified using the Hs00203958_ml TaqMan gene expression assay (Applied Biosystems) according to the protocol provided by the manufacturer. A plasmid containing the full-length *FoxP3* insert was used to generate standard curves.

*Statistics*. T cell analysis before and after treatment was performed by IFN-γ ELISPOT on all patients who completed immunotherapy. Increases of antigen-specific $CD4^+$ and $CD8^+$ T cells after vaccination were compared using the Wilcoxon matched-pairs signed rank test, analyzing the null hypothesis that the rates of change in T cell response were equivalent prior to and after therapy. A 2-sided $P$ value of less than 0.05 was considered statistically significant.

## Acknowledgments

This work was supported in part by NIH grants R21-CA098446-02 (National Cancer Institute) and M01-RR-30 (National Center for Research Resources, General Clinical Research Centers Program). We would like to thank Ligand Pharmaceuticals for provision of the fusion protein for the clinical study.

Received for publication June 13, 2005, and accepted in revised form October 4, 2005.

Address correspondence to: Johannes Vieweg, Duke University Medical Center, MSRB, Suite 455, DUMC Box 2626, Durham, North Carolina 27710, USA. Phone: (919) 684-9949; Fax: (919) 681-7414; E-mail: j.vieweg@duke.edu.

1. Su, Z., et al. 2003. Immunological and clinical responses in metastatic renal cancer patients vaccinated with tumor RNA-transfected dendritic cells. *Cancer Res.* **63**:2127–2133.
2. Heiser, A., et al. 2002. Autologous dendritic cells transfected with prostate-specific antigen RNA stimulate CTL responses against metastatic prostate tumors. *J. Clin. Invest.* **109**:409–417. doi:10.1172/JCI200214364.
3. Shevach, E.M. 2001. Certified professionals: CD4(+)CD25(+) suppressor T cells. *J. Exp. Med.* **193**:F41–F46.
4. Jonuleit, H., Schmitt, E., Schuler, G., Knop, J., and Enk, A.H. 2000. Induction of interleukin 10-producing, nonproliferating CD4(+) T cells with regulatory properties by repetitive stimulation with allogeneic immature human dendritic cells. *J. Exp. Med.* **192**:1213–1222.
5. Read, S., and Powrie, F. 2001. CD4(+) regulatory T cells. *Curr. Opin. Immunol.* **13**:644–649.
6. Woo, E.Y., et al. 2002. Cutting edge: regulatory T cells from lung cancer patients directly inhibit autologous T cell proliferation. *J. Immunol.* **168**:4272–4276.
7. Curiel, T.J., et al. 2004. Specific recruitment of regulatory T cells in ovarian carcinoma fosters immune privilege and predicts reduced survival. *Nat. Med.* **10**:942–949.
8. Shimizu, J., Yamazaki, S., and Sakaguchi, S. 1999. Induction of tumor immunity by removing CD25+CD4+ T cells: a common basis between tumor immunity and autoimmunity. *J. Immunol.* **163**:5211–5218.
9. Onizuka, S., et al. 1999. Tumor rejection by in vivo administration of anti-CD25 (interleukin-2 receptor alpha) monoclonal antibody. *Cancer Res.* **59**:3128–3133.
10. Sutmuller, R.P., et al. 2001. Synergism of cytotoxic T lymphocyte-associated antigen 4 blockade and depletion of CD25(+) regulatory T cells in antitumor therapy reveals alternative pathways for suppression of autoreactive cytotoxic T lymphocyte

responses. *J. Exp. Med.* **194**:823–832.
11. Frankel, A.E., Powell, B.L., and Lilly, M.B. 2002. Diphtheria toxin conjugate therapy of cancer. *Cancer Chemother. Biol. Response Modif.* **20**:301–313.
12. Takahashi, T., et al. 1998. Immunologic self-tolerance maintained by CD25+CD4+ naturally anergic and suppressive T cells: induction of autoimmune disease by breaking their anergic/suppressive state. *Int. Immunol.* **10**:1969–1980.
13. Waldmann, T.A. 1991. The interleukin-2 receptor. *J. Biol. Chem.* **266**:2681–2684.
14. Wing, K., Ekmark, A., Karlsson, H., Rudin, A., and Suri-Payer, E. 2002. Characterization of human CD25+ CD4+ T cells in thymus, cord and adult blood. *Immunology.* **106**:190–199.
15. Read, S., et al. 1998. CD38+ CD45RB(low) CD4+ T cells: a population of T cells with immune regulatory activities in vitro. *Eur. J. Immunol.* **28**:3435–3447.
16. Thornton, A.M., and Shevach, E.M. 2000. Suppressor effector function of CD4+CD25+ immunoregulatory T cells is antigen nonspecific. *J. Immunol.* **164**:183–190.
17. Morgan, M.E., et al. 2005. Expression of FOXP3 mRNA is not confined to CD4+CD25+ T regulatory cells in humans. *Hum. Immunol.* **66**:13–20.
18. Woo, E.Y., et al. 2001. Regulatory CD4(+)CD25(+) T cells in tumors from patients with early-stage non-small cell lung cancer and late-stage ovarian cancer. *Cancer Res.* **61**:4766–4772.
19. Rosolen, A., et al. 1989. Expression of interleukin-2 receptor beta subunit in hematopoietic malignancies. *Blood.* **73**:1968–1972.
20. Olsen, E., et al. 2001. Pivotal phase III trial of two dose levels of denileukin diftitox for the treatment of cutaneous T-cell lymphoma. *J. Clin. Oncol.* **19**:376–388.
21. Jonuleit, H., Schmitt, E., Steinbrink, K., and Enk, A.H. 2001. Dendritic cells as a tool to induce anergic and regulatory T cells. *Trends Immunol.* **22**:394–400.
22. Heiser, A., et al. 2000. Human dendritic cells transfected with RNA encoding prostate specific antigen stimulate prostate specific CTL responses in vitro. *J. Immunol.* **164**:5508–5514.
23. Heiser, A., et al. 2001. Human dendritic cells transfected with renal tumor RNA stimulate polyclonal T-cell responses against antigens expressed by primary and metastatic tumors. *Cancer Res.* **61**:3388–3393.
24. Heiser, A., et al. 2001. Induction of polyclonal prostate cancer specific cytotoxic T lymphocytes using dendritic cells transfected with amplified tumor RNA. *J. Immunol.* **166**:2953–2960.
25. Baecher-Allan, C., Viglietta, V., and Hafler, D.A. 2002. Inhibition of human CD4(+)CD25(+high) regulatory T cell function. *J. Immunol.* **169**:6210–6217.
26. Su, Z., et al. 2005. Telomerase mRNA-transfected dendritic cells stimulate antigen-specific CD8+ and CD4+ T cell responses in patients with metastatic prostate cancer. *J. Immunol.* **174**:3798–3807.
27. Goldrath, A.W., Luckey, C.J., Park, R., Benoist, C., and Mathis, D. 2004. The molecular program induced in T cells undergoing homeostatic proliferation. *Proc. Natl. Acad. Sci. U. S. A.* **101**:16885–16890.
28. Tsaknaridis, L., et al. 2003. Functional assay for human CD4+CD25+ Treg cells reveals an age-dependent loss of suppressive activity. *J. Neurosci. Res.* **74**:296–308.

# Appendices B

**Reversal of myeloid cell-mediated immunosuppression in patients with metastatic renal cell carcinoma**

Sergei Kusmartsev[1], Zhen Su[1], Axel Heiser[1], Jens Dannull[2], Evgeniy Eruslanov[1], Hubert Kübler[1], Donna Yancey[2], Philip Dahm[1], Johannes Vieweg[1]

[1]Department of Urology, College of Medicine, University of Florida, Gainesville, Florida; [2]Department of Surgery, Duke University Medical Center, Durham, North Carolina

**This work was supported by US Army, Department of Defense (W81XWH-05-1-0011)**

**Correspondence:**

Johannes Vieweg, M.D.

Department of Urology

University of Florida, College of Medicine

Room N2-3, Health Science Center

P.O. Box 100247

Gainesville, Florida 32610-0247

Tel: (352) 392-4504

Fax: (352)-73-83-35

E-mail: j.vieweg@urology.ufl.edu

## STATEMENT OF CLINICAL RELEVANCE

Many studies have shown that the growth of cancers including renal cell carcinoma (RCC) is often associated with a decline in immune function and therapeutic vaccines alone are often ineffective to overcome tumor-mediated immune suppression. Previous studies have highlighted the role of myeloid-derived suppressor cells (MDSC) in cancer-associated immune non-responsiveness in patients with metastatic RCC. Accumulation of these cells in tumor hosts is promoted by tumor-derived factors and this tumor-driven expansion of MDSC contributes to tumor escape from the immune system. In this study we analyzed the mechanisms by which MDSC inhibit T cell responses and demonstrate a reversal of this effect by ATRA treatment. Our results suggest that ATRA treatment could help in the depletion of these immunosuppressive cells; however, more studies are needed to find the most optimal individual approach to improve the effect of cancer vaccination.

**ABSTRACT**

**Purpose**: Tumor-induced immunosuppression remains a significant obstacle limiting the efficacy of biologic therapy of renal cell carcinoma (RCC). Here we evaluate the role of CD33 myeloid-derived suppressor cells (MDSC) in regulation of T cell responses in RCC patients. We also examine effect of all-trans-retinoic acid (ATRA) on MDSC-mediated immune suppression.

**Experimental Design**: CD33-positive cells were isolated from RCC patients with magnetic beads and tested in vitro for its ability to inhibit T cell responses. To evaluate whether in vivo ATRA treatment could diminish immune suppression in RCC patients, a separate clinical trial has been designed. ATRA in capsules (Tretinoin) was given to patients for 7 consecutive days. After ATRA administration patients were given six intradermal injections of cancer vaccine - hTERT mRNA-transfected dendritic cells. Immunologic response to cancer vaccine was evaluated using ELISPOT assay.

**Results:** MDSC isolated from RCC patients, but not from healthy donors, were capable of suppressing antigen specific T-cell responses in vitro through secretion of reactive oxygen species and nitric oxide upon interaction with cytotoxic T cells (CTL). MDSC-mediated immune suppression and interferon-gamma down-regulation was reversible in vitro by exposing cells to the ROS inhibitors. Moreover, ATRA was capable of abrogating MDSC-mediated immunosuppression and improving T-cell function by direct differentiation into APC precursors. Administration of ATRA to metastatic RCC patients significantly reduced MDSC-mediated immunosuppression and T cell reactivity.

**Conclusions**: These results may have significant implications regarding the future design of active immunotherapy protocols that may include differentiation agents as part of a multimodal approach to RCC immunotherapy.

## INTRODUCTION

The incidence of renal cell carcinoma (RCC) is rising with approximately 35,000 new cases detected annually in the U.S. Like melanoma, RCC has shown to respond to immunotherapeutic intervention; however tumors are capable of evading immune recognition, thus limiting the efficacy of biologic therapy (1-3). Previous studies have shown that secretion of tumor-mediated factors such as VEGF, TGF-β, GM-CSF, and $PGE_2$ results in altered hematopoiesis and accumulation of myeloid-derived suppressor cells (MDSC) in the tumor-bearing host(4-11). MDSC have shown to interfere with the differentiation, function and survival of antigen presenting (APC) and effector T cells by utilizing enzymes involved in arginine metabolism, namely inducible nitric oxide synthase which generates nitric oxide, and arginase I, which acts by L-arginine depletion (12-14). Moreover, MDSC produce elevated levels of reactive oxygen species (ROS)(15, 16) and trigger T-cell tolerance through T-cell-receptor dependent or independent mechanisms(17-19). Although several studies have analyzed the phenotype and function of MDSC in murine systems, much less is known regarding the relevance and immunosuppressive action of MDSC in cancer patients.

In this study, we found that the frequencies of $CD33^+HLA\text{-}DR^-$ MDSC isolated from the peripheral blood of patients with metastastic (RCC) are significantly elevated when compared to $CD33^+HLA\text{-}DR^-$ cells from healthy donors. MDSC isolated from peripheral blood of RCC patients, but not from healthy donors, were capable of suppressing antigen specific T-cell responses in vitro through secretion of reactive oxygen species (ROS) and nitric oxide upon interaction with cytotoxic T cells (CTL). MDSC-mediated immune suppression and interferon-γ downregulation was reversible by adding the ROS inhibitors catalase and superoxide dismutase to MDSC. Moreover, all-trans retinoic acid (ATRA) was capable of abrogating MDSC-mediated

immunosuppression and improving T-cell function by direct differentiation into APC precursors. Administration of ATRA to metastatic RCC patients significantly reduced MDSC-mediated immunosuppression and improved T-cell reactivity. These results may have significant implications regarding the future design of active immunotherapy protocols that may include differentiation agents as part of a multimodal approach to the immunotherapy of RCC patients.

## MATERIALS AND METHODS

### *Biologic Samples.*

Peripheral blood was collected from patients with diagnosis of a metastatic renal cell carcinoma stage III-IV ($pT_4N_xM_x$) and healthy donors through the Department of Urology at University of Florida, Gainesville, FL and Department of Surgery, at Duke University Medical Center (Duke University, Durham, NC). All specimens were obtained after informed consent and approval by the institutional review boards. Excluded from the study were patients with: central nervous system metastases; a history of autoimmune disease; serious intercurrent chronic or acute illnesses; concurrent second malignancy other than nonmelanoma skin cancer; or controlled superficial bladder cancer. Also excluded were patients on immunosuppressive agents. Donors and patients age have been matched. Peripheral blood mononuclear cells (PBMC) were separated by Histopaque gradient centrifugation.

***Reagents and antibodies.*** The MART-1-specific CTL clone which was originally obtained from S.A. Rosenberg (NCI, Bethesda, MD) and kindly provided by S.K. Pruitt (Department of Surgery, Duke University, Durham). MART-$1_{26–35}$ native peptide (EAAGIGILTV) and MART-$1_{26–35}$ A27L peptide analogue (ELAGIGILTV) were synthesized by New England Peptides Inc (Boston, MA).GM-CSF was obtained from Immunex (Seattle, WA). Dichlorodihydrofluorescein diacetate (DCFDA) and 4-amino-5-methylamino-2', 7'-difluorescein (DAF-FM) were purchased from Molecular Probes (Eugene, OR). Superoxide dismutase (SOD), catalase and uric acid were purchased from Calbiochem (La Jolla, CA). Tetanus toxoid was purchased from List Biological Labs (Campbell, CA). ATRA (Tretinoin) was obtained from Roche Pharmaceuticals (Nutley, NJ). $^{51}Cr$ and $^{3}H$-thymidine were from Amersham-Buchler (Braunschweig, Germany). The following fluorochrome-conjugated antibodies were used for flow cytometry: HLA-DR, HLA-

ABC, CD1a, CD3, CD10, CD11c, CD13, CD14, CD15, CD16b, CD18, CD19, CD31,CD33, CD40, CD56,CD86, CD115 (all from BD Pharmingen (San Diego, CA) or Caltag Laboratories (Burlingame, CA).

***Isolation of CD33$^+$HLA-DR$^-$ cells.*** CD33$^+$HLA-DR$^-$ cells were isolated from peripheral blood of RCC patients using MACS microbeads and columns (Miltenyi Biotec, Auburn, CA). Briefly**,** freshly isolated PBMC were resuspended in cold MACS buffer and incubated with HLA-DR microbeads (Miltenyi Biotec, Auburn, CA) for 15 min on ice. Then cells were washed with cold MACS buffer to remove unbound beads and subsequently subjected to depletion of HLA-DR$^+$ cells on a MACS column according to the manufacturer's instructions (Miltenyi Biotec, Auburn, CA). The negative cell fraction was collected, washed and then incubated with CD33 microbeads. MACS column was used for positive selection of CD33$^+$HLA-DR$^-$ cells. The purity of the CD33$^+$ cell population was evaluated by flow cytometry and exceeded 90%.

***Flow cytometry.*** A total of $1 \times 10^6$ cells were suspended in PBS buffer and incubated for 20 minutes at 4°C with the antibody and then washed twice with cold PBS. Fluorochrome-conjugated antibodies as well as isotype control antibodies were used for cell staining. Non-specific staining was prevented by blocking Fc receptors**.** To block Fc receptors cells were incubated for 5 min at $4^0$ C with anti-CD16/CD32 mAbs. FACS data were acquired using a FACSCalibur flow cytometer (BD Biosciences, San Jose, CA) and were analyzed using CellQuest software (BD Biosciences). Results were expressed as the percentage of positive cells and mean fluorescence intensity.

***ELISPOT assay.*** To test whether CD33$^+$HLA-DR$^-$ myeloid cells are capable of inhibiting a CD8 T cell response we used ELISPOT assay. Briefly, freshly isolated myeloid cell subsets from HLA-A0201-positive cancer patient or from healthy donor were pulsed with MART-1 peptide

and incubated with MART-1 specific CTL clone at a ratio of 1:1. A cell mixture of $CD33^{+}HLA\text{-}DR^{-}$ cells, CTLs and T2 cells (loaded with peptide) was added to 96-well plates for ELISPOT (Millipore, Billerica, MA), which were pre-coated with 2 μg/ml IFN-γ capture antibody. Plates were incubated for 20 hours at 37°C, and biotinylated IFN-γ detection antibody was added to each well. Cells were then incubated for an additional 2 hours at room temperature, then with streptavidin-alkaline phosphatase (1 μg/ml; Sigma-Aldrich); plates were developed with substrate (Kirkegaard & Perry Laboratories, Gaithersburg, MD). After washing, spots were counted using an automated ELISPOT counter.

***CTL assay.*** For CTL assay, HLA-A201-restricted MART-1-specific CTLs (MART-1 CTL clone), were cultured for 5h with $^{51}Cr$-labeled, MART-1 peptide-loaded T2 target cells at a 1:1 ratio. Similar numbers of $CD33^{+}HLA\text{- }DR^{-}$ (pulsed with peptide) cells from HLA-A201-positive RCC patients, or control $CD33^{+}HLA\text{-}DR^{-}$ (pulsed with peptide) from healthy control donors, were then added to wells containing effector/target cells. As controls, peptide-loaded T2 cells (Cold Target), were added to individual cultures. Target cells were labeled with 200 μCi of $NaCrO_4$ (Amersham-Buchler, Braunschweig, Germany) in 0.5 ml of complete medium for 1 h. They were washed three times with complete medium and added at a concentration of $5x10^3$ cells/per well in round-bottom microplates. Effector cells were added at various E:T cell ratios in a final volume of 200 μl/well. The plates were incubated for 4 h at 37°C in a humid atmosphere with 5% $CO_2$. Maximum chromium release was ensured by the addition of 10% Triton-X, and spontaneous release was assessed by adding complete medium (RPMI 1640 plus 10% FCS) to the target cells. The culture supernatant was harvested semi-automatically with a Scatron Titertek System (Scatron, Suffolk, U.K.) and counted in a gamma counter (Beckmann, Heidelberg,

Germany). The percentage of specific lysis was calculated as [(experimental cpm - spontaneous cpm)/(maximum cpm - spontaneous cpm)] x 100. All determinations were made in triplicate.

***Production of reactive oxygen species (ROS) and nitric oxide (NO).*** Oxidation-sensitive dye dichlorodihydrofluorescein diacetate ($H_2$DCFDA) and NO-specific fluorogenic probe 4-amino-5-methylamino-2', 7'-difluorescein (DAF-FM) were used for the measurement of ROS and NO production, respectively, by $CD33^+$ myeloid cells. Freshly isolated $CD33^+$HLA- $DR^-$ cells from an HLA-A0201-positive RCC patients (or healthy donors) were pulsed with MART-1 peptide, loaded with $H_2$DCFDA (5 μM) or DAF-FM (5 μM), and then incubated with a MART-1 specific CTL clone for 1 h (at a cell ratio of 1:1). After washing with cold PBS, CD3-negative cells were gated and analyzed by flow cytometry.

***RT-PCR.*** Total RNA was isolated using TRIZOL reagent (Invitrogen). Reverse transcription was performed at 25°C for 10 min, 42°C for 2 h, and 72°C for 5 min from 100 ng of total RNA using Superscript II reverse transcriptase (Invitrogen) and random primers (3 μg/μl; Invitrogen).

***Treatment of patients with Tretinoin (ATRA) in combination with cancer vaccine.*** To evaluate whether *in vivo* ATRA treatment could diminish immune suppression mediated by MDSC and improve the immune response of vaccinated RCC patients, we designed a separate clinical trial**.** Patients with histologically confirmed metastatic RCC were eligible for this study. Treatment of patients was performed following written informed consent as part of a protocol approved by an Institutional Review Board and the FDA. ATRA in capsules was given to patients for 7 consecutive days in a dose of 80 mg/day. ATRA (Tretinoin) is an FDA approved compound manufactured by Roche Pharmaceuticals for the treatment of Acute Promyelocytic Leukemia (APL). Virtually all patients experience some drug-related toxicity associated with the administration of ATRA (Tretinoin), especially headache, fever, weakness and fatigue. These

adverse effects are rarely permanent or irreversible nor do they usually require interruption of therapy. After ATRA administration patients were given six intradermal injections of cancer vaccine - hTERT mRNA-transfected DC. Preparation of hTERT mRNA-transfected DC was done as described before (20). The injections of DC were given at weekly intervals and consisted of 1 x $10^7$ cells suspended in 200 µl of 0.9% sodium chloride (Abbott Laboratories) at each vaccination cycle as described earlier (21). Follow-up visits occurred biweekly for three visits, then every 2 months or until the subject was removed from the study.

***Statistical analysis.*** The statistical significance between values was determined by the Student *t* test. All data were expressed as the mean ± SD. Probability values ≥ 0.05 were considered non-significant. Flow cytometry data shown are representative of at least two separate determinations.

## RESULTS

### Isolation of $CD33^{+}HLA\text{-}DR^{-}$ myeloid cell populations

For initial phenotypic analysis of MDSC in the peripheral blood of RCC patients we adapted techniques described previously(22). We isolated PBMC from RCC patients and control healthy donors and then analyzed for presence of lineage negative/HLA-DR negative cell populations ($Lin^{-}/DR^{-}$). As shown in Fig.1A and 1B, number of $Lin^{-}HLA\text{-}DR^{-}$ cells was significantly increased in cancer patients Subsequently, $Lin^{-}/DR^{-}$ cells were analyzed for cell surface expression of CD1a, CD10, CD11b, CD13, CD114, CD18, CD31, CD33, HLA ABC and HLA-DR. As shown in Figure 1C, $Lin^{-}/DR^{-}$ cells exhibited high expression levels of HLA class I, CD18, CD33, and intermediate cell surface expression for CD1a, CD10, CD13, CD31 and CD11b, consistent with the MDSC phenotype previously described (22).

Since most of $Lin^{-}HLA\text{-}DR^{-}$ MDSC expressed CD33, we developed an isolation method of MDSC peripheral blood of cancer patients using CD33 as positive selection marker. PBMC from RCC patients and healthy donors were first depleted of HLA-DR-positive cells and then subsequent positive selection of CD33-positive cell population resulted in depletion exhibiting high expression of HLA class I in both donor and RCC samples. Practically all isolated CD33 MDSC also co-expressed CD11b (Fig. 2A, upper right panel), and only minor portion of these cells (16%) expressed granulocytic marker CD114 (Fig. 2A, lower right panel). CD115, the receptor for CSF-1 (macrophage colony stimulating factor) was only expressed in RCC-derived $CD33^{+}HLA\text{-}DR^{-}$ MDSC (data not shown). Cytologic analysis of $CD33^{+}$ cells revealed the heterogeneous cell morphology consisting of two major cell types including mononuclear ”monocytic” cells with one large nucleus and polymorphonuclear “granulocytic” cells with segmented nuclei (Figure 2B). It should be noted that proportion of “monocytic” and

"granulocytic" cell types in among CD33 MDSC has varied from patient to patient. In summary we show that the myeloid marker CD33 can be used for isolating and enumerating MDSC from the PBMC of RCC patients and that $CD33^{+}HLA\text{-}DR^{-}$ MDSC are significantly elevated in cancer patients but not healthy volunteers.

**Functional analysis of $CD33^{+}HLA\text{-}DR^{-}$ myeloid cells**

We next evaluated the functional capacity of $CD33^{+}HLA\text{-}DR^{-}$ myeloid cells to suppress antigen-specific T-cell responses using Interferon-γ ELISPOT analysis. $CD33^{+}$ MDSC from a HLA-A0201-positive cancer patient or from a healthy donor were pulsed with MART-1 peptide and incubated with MART-1 specific CTL clone at ratio of 1:1. As shown in Fig. 3A, the addition of RCC patient-derived, but not from donor-derived $CD33^{+}HLA\text{-}DR^{-}$ cells to the ELISPOT reaction, significantly suppressed the numbers of interferon-γ secreting effector T cells. In separate experiments, we tested whether $CD33^{+}HLA\text{-}DR^{-}$ cells are capable of suppressing CTL activity and T-cell proliferation. As shown in Fig. 3B, $CD33^{+}HLA\text{-}DR^{-}$ cells from RCC patients significantly inhibited lysis of T2 tumor target cells mediated by MART-1 specific CTLs. Additionally, RCC-derived myeloid cells efficiently inhibited tetanus toxoid (TT)-induced proliferation of T cells from healthy donors (Fig. 3C).

It has been previously reported that production of IFN-gamma by T cells in response to antigenic stimuli is regulated by reactive oxygen species that are produced by MDSC derived from cancer patients(15) or tumor-bearing mice(23). To test whether reactive oxygen species are involved in inhibition of T cell responses by $CD33^{+}HLA\text{-}DR^{-}$ myeloid cells, we used specific inhibitors of ROS production (Fig. 4A). The addition of catalase [500 U/ml] significantly reduced MDSC-mediated T-cell suppression, suggesting that $H_2O_2$ contributes to MDSC-mediated T-cell inhibitory function. Superoxide dismutase (SOD), which converts superoxide anion into

hydrogen peroxide) alone did not significantly reverse myeloid cell-mediated immune suppression; however the combination of catalase and SOD reversed immune suppression in a synergistic fashion.

Since the production of ROS was responsible for T cell inhibition, we further, in a separate experiment, sought to answer whether direct interaction between $CD33^{+}HLA\text{-}DR^{-}$ myeloid suppressor cells (loaded with antigen) and antigen-specific T cells could promote burst of ROS production. Therefore, we incubated MART-1 peptide pulsed CD33-positive myeloid cells with a MART-1 peptide specific CTL clone and subsequently stained these cells with the fluorogenic ROS-sensitive probe dichlorodihydrofluorescein diacetate ($H_2$DCFDA). As shown in Figure 4, panel C, isolated from RCC patient constitutively produced ROS, and its production was further enhanced after co-culture with CTL. In contrast, only low levels of ROS production could be detected in a similar control cell population ($CD33^{+}HLA\text{-}DR^{-}$) cells isolated from a healthy donor) after co-culture with MART-1 specific CTL that only insignificantly increased after antigen-specific stimulation. Thus, consistent with the experiments shown in Figure 4A and 4B, RCC patient-derived CD33-positive cells constitutively produced ROS and its levels were greatly enhanced after co-culture with T cells.

Since nitric oxide has also been shown to be involved in mechanisms of MDSC-mediated immune suppression(8, 24-26), we measured NO production by $CD33^{+}HLA\text{-}DR^{-}$cells using the same experimental conditions described above. For detection of NO produced by myeloid cells, the fluorogenic diacetate (4-amino-5-methylamino-2', 7'-difluorescein (DAF-FM) was used. DAF-FM diacetate, is a cell permeable molecule that forms a fluorescent product benzotriazole after reaction with endogenous NO (27). We found that $CD33^{+}HLA\text{-}DR^{-}$ cells derived from cancer patients but not from healthy donors constitutively produce substantial levels of NO (Fig.

4D). Moreover, NO production can be further enhanced by MDSC upon interaction with CTLs in a antigen-specific manner. In summary, we show here that ROS and NO are major factors contributing to T-cell suppression mediated by $CD33^{+}HLA\text{-}DR^{-}$ myeloid suppressor cells. In RCC patients, both ROS and NO production increased significantly after antigen-specific T-cell interaction, while in healthy volunteer-derived, no significant production of ROS or NO could be observed.

### *In vitro* and *in vivo* effect of ATRA on immune suppression mediated by $CD33^{+}HLA\text{-}DR^{-}$ cells

ATRA is a naturally occurring metabolite of vitamin A. it is capable of inducing the differentiation of the leukemic cell line HL6020(28) and is clinically used for induction therapy of patients with acute promyelocytic leukemia. It has also previously been shown that ATRA can promote differentiation of human immature myeloid cells into monocyte/macrophages and dendritic cells (22, 29). Murine studies suggested that ATRA can significantly decrease numbers of MDSC in the tumor-bearing host by promoting its differentiation into a mature $CD11c^{+}$ DC, thereby improving the efficacy of the cancer vaccination (30). Therefore, we investigated whether ATRA could promote *in vitro* differentiation of $CD33^{+}HLA\text{-}DR^{-}$ myeloid suppressor cells derived from cancer patients and reduce/or revert its inhibitory effects on T cells.

Since ATRA binds to specific receptors, we first measured expression of RAR-α, RAR-β and RAR-γ retinoic acid receptors in MDSC derived from RCC patients. As shown in Fig. 5A, RCC-derived MDSC population has increased expression of RAR-γ. We next asked whether ATRA can reduce the T cell inhibition mediated by $CD33^{+}HLA\text{-}DR^{-}$ myeloid suppressor cells. CTL assay was performed in the presence of MDSC isolated from an RCC patient as described in

Materials and Methods. As shown in Fig 6A, MART-1 peptide-loaded $CD33^{+}HLA\text{-}DR^{-}$ cells, isolated from a RCC patient, significantly inhibited lysis by MART-1-specific CTL, while the same cell population from healthy donor-derived exhibited only a modest T-cell suppressive function. Exposure of MDSC to ATRA [1μM] was capable of abrogating the immunosuppressive effect of $CD33^{+}HLA\text{-}DR^{-}$ cells. Thus, $CD33^{+}$ MDSC significantly inhibited antigen-specific CTL responses *in vitro*, but their immunosuppressive action could be reversed by presence in culture of ATRA.

To evaluate the effect of ATRA on *in vitro* differentiation of MDSC, PBMC from RCC patient were subjected to HLA-DR and CD15 negative depletion, followed by positive selection for CD33 marker. After 4 days of culture in GM-CSF-containing media supplemented with or without 1μM ATRA the phenotype of isolated cells was analyzed by FACS. Figure 6B shows that presence of ATRA in culture could significantly improve GM-CSF-induced differentiation of $CD33^{+}HLA\text{-}DR^{-}$ myeloid cells as evidenced by enhanced acquisition of the cell surface markers CD1a, HLA-DR and CD40. Taken together, we have shown that *in vitro* culture of $CD33^{+}HLA\text{-}DR^{-}$ myeloid suppressor cells with ATRA abrogates its immune suppressive effect on T cell function through promoting of APC differentiation and up-regulating of MHC class II and costimulatory molecules.

To test whether *in vivo* administration of ATRA would benefit RCC patients, reduce MDSC-mediated immune suppression and improve effect of cancer vaccination, we designed a separate clinical trial. To date, three RCC patients were enrolled in this study. Patients were given ATRA for 7 days and then received DC vaccines (see *Materials and Methods*). Two weeks after last vaccination, we isolated the $CD33^{+}$ cells and tested their ability to inhibit production of IFN-gamma by T cells. Since treated patients were HLA-A2 negative, IFN-gamma production was

measured by ELISA. MART-1 peptide-loaded T2 cells and a MART-1-specific CTL clone (ratio 1:1) were co-incubated with increasing numbers of MDSC overnight and supernatants were analyzed for interferon-gamma content (Fig. 7). The obtained results revealed that ATRA administration in cancer patients lead to significant reduction of inhibitory activity of myeloid suppressive cells on T cell immune response in two out of three treated patients

## DISCUSSION

Many studies have shown that the growth of cancers including RCC is often associated with a decline in immune function and therapeutic vaccines alone are often ineffective to overcome tumor-mediated immune suppression. Also, most vaccination strategies lack sufficient activity to counteract antigen-specific immune tolerance and to generate a potent and durable T-cell response in cancer patients (3, 31, 32). Previous studies have highlighted the role of MDSC in cancer-associated immune non-responsiveness (reviewed in (33). Accumulation of these cells in tumor hosts is promoted by tumor-derived factors and this tumor-driven expansion of MDSC contributes to tumor escape from the immune system. Recently Mirza et al. showed that ATRA treatment of patients with RCC reduced the number of MDSC and improved T cell proliferation after antigen stimulation (29). In this study we analyzed the mechanisms by which MDSC inhibit T cell responses and demonstrate a reversal of this effect by ATRA treatment.

We show that the proportion of $Lin^{-}HLA\text{-}DR^{-}$ myeloid cells is considerably elevated in the peripheral blood of RCC patients, when compared to healthy volunteers. These cells display characteristics of immature myeloid cells consistent with the MDSC phenotype previously described by Almand and coworkers and are capable of inhibiting of T cell(29). Importantly, these cells also express myeloid cell marker CD33. We demonstrate that the MDSC population

from RCC patients could be enriched via isolation of $CD33^{+}HLA\text{-}DR^{-}$cells. Consistent with the data shown in Figures 1 and 2, $CD33^{+}HLA\text{-}DR^{-}$ MDSC represent a homogeneous cell population that is significantly elevated in RCC patients when compared to healthy volunteers. Purified $CD33^{+}$ myeloid cells from RCC patients are characterized by considerable T-cell suppressive activity *in vitro*. Thus, $CD33^{+}HLA\text{-}DR^{-}$ cells derived from RCC patients inhibit PHA-induced T cell proliferation in dose-dependent manner. In order to provide evidence that $CD33^{+}HLA\text{-}DR^{-}$ MDSC are also capable of inhibiting antigen-specific $CD8^{+}$ T-cell responses, we tested their immunosuppressive activity in CTL and interferon-γ ELISPOT assay using isolated and peptide-loaded $CD33^{+}$ cells from an $HLA\text{-}A2^{+}$ RCC patient. MART-1 peptide-loaded MDSC significantly inhibited CTL-mediated lysis (Fig. 6) or interferon-γ secretion (Fig. 4) in an antigen-specific fashion while the control peptide-loaded MDSC, MART-1 peptide-loaded healthy donor MDSC and unloaded T2 cells exhibited no or only modest inhibitory activity. These results support the notion that freshly-derived $CD33^{+}HLA\text{-}DR^{-}$ MDSC show significant T cell inhibitory potential.

It has been previously established that MDSC derived from cancer patients as well as from tumor-bearing mice produce high levels of reactive e oxygen species (ROS)(15). Moreover, via production of ROS the tumor-derived myeloid cells can regulate T cell responses. In order to evaluate the contribution of ROS in MDSC-mediated mechanisms of T cell inhibition in RCC patients, purified CD33+ cells were pulsed with MART-1 peptide, loaded with DCFDA and then cultured with MART-1- specific CTLs. Obtained results show that 1) $CD33^{+}$ myeloid cells derived from RCC patients constitutively produced ROS, while no significant production was observed in their cell counterparts isolated from healthy donors; 2) production of ROS by $CD33^{+}$ cells was increased upon antigen-specific contact of myeloid cells with T cells; 3) inhibition of

IFN-gamma production by T cells by $CD33^{+}HLA\text{-}DR^{-}$ cells could be abrogated by specific ROS scavengers such as catalase. Another characteristic of $CD33^{+}HLA\text{-}DR^{-}$ MDSC is production of nitric oxide. Again, these myeloid cells derived from RCC patients but not from healthy donors constitutively produced NO. The amount of NO production was substantially increased by CD33-positive cells after contact with T cells.

Interestingly that all characteristics indicated above of $CD33^{+}HLA\text{-}DR^{-}$ suppressive cells (such as ability to inhibit T cell proliferation and CTL activity, increased production of ROS and nitric oxide upon contact with activated T cells) are similar to the MDSC population (Gr-1+CD11b+ cells) whose expansion is described in various murine tumor models (8, 34). Moreover, similar to MDSC-derived from animal tumor hosts, $CD33^{+}$ MDSC are precursors of APC since they are capable of differentiating *in vitro* into mature antigen-presenting cells after culture in presence of GM-CSF (16, 34). Taken together, these results support the hypothesis that cancers in humans and animals may use the same or similar mechanisms to evade the immune system. The accumulation of immune suppressive cells in cancer patients favors conditions that allow tumors to escape immune recognition and promote progressive growth of malignant cells.

Among the strategies that can overcome MDSC-mediated immune suppression is the use of differentiation agents, such as ATRA. ATRA promotes *in vitro* differentiation of MDSC into mature APC (22, 29). Studies in mice suggest that systemic treatment with ATRA is capable of reducing the frequencies of MDSC, thereby abrogating their inhibitory activity *in vivo* (30). ATRA-mediated reduction of MDSC improved both $CD4^{+}$ and $CD8^{+}$ T-cell responses and significantly enhanced the efficacy of the cancer vaccination. These findings form a rationale to augment a vaccine-induced T-cell response with pre-treatment of ATRA that can lead to the reduction or elimination of MDSC in cancer patients. In present study we tested the effect of

ATRA on *in vitro* differentiation of $CD33^+$ myeloid cells derived from RCC patients as well on their immune suppressive potential. We show that the addition of ATRA enhances GM-CSF–stimulated differentiation which results in the acquisition of HLA-DR and costumulatory molecules (CD40). Furthermore, presence of ATRA abrogated the immune suppressive effect of $CD33^+$ cells on T cell response presumably by promoting myeloid cell differentiation. In separate experiments we measured expression of nuclear retinoic acid receptors (RAR) by immune suppressive cells by RT-PCR. These cells express high levels of RAR-alpha and RAR-γ, however RAR-beta expression was almost negligible. Finally, we tested whether ATRA administration could reverse or reduce the cancer-associated immune suppression that was mediated by MDSC. Our results demonstrate that $CD33^+$HLA- $DR^-$ MDSC from patients treated with ATRA show reduced inhibitory activity on T cell function.

Cumulatively, we have identified that $CD33^+$HLA-$DR^-$ cells in RCC patients represent a MDSC population. Additionally we have shown that ROS and NO are major mechanisms by which MDSC inhibit a T cell response. MDSC may greatly contribute to immune evasion thus promoting tumor growth. These cells represent a significant obstacle for cancer immune therapy because they may inhibit the vaccine-induced T cell response. Therefore, there is considerable interest in developing strategies that allow targeting and eliminating MDSC in immunotherapy protocols. Our results suggest that ATRA treatment could help in the depletion of these suppressor cells; however, more studies are needed to find the most optimal individual approach to improve the effect of cancer vaccination.

**Acknowledgements:** The authors would like to thank Susan Fesperman for the editorial assistance. Some of the studies referred to in this manuscript were in part supported by NIH K24, VA MERIT review grant and the National Center for Research Resources, (MO1-RR-30), General Clinical Research Centers Program.

References


1. Rosenberg SA, Yang JC, Restifo NP. Cancer immunotherapy: moving beyond current vaccines. Nat Med 2005;10: 909-15
2. Deerwish IH, Tannebaum CS, Rayman PA, Finke JH. Mechanisms of immune dysfunction in renal cell carcinoma. Cancer Treat Res 2003;116: 29-51.
3. Vieweg J, Jackson A. Antigenic targets for renal cell carcinoma immunotherapy. Exp Opin Biol Ther 2004;4: 1791-801.
4. Young MRI, Wright MA, Matthews JP, Malik I, Prechel M. Suppression of T cell proliferation by tumor-induced granulocyte-macrophage progenitor cells producing transforming growth factor- β and nitric oxide J Immunol 1996;156:: 1916-21.
5. Gabrilovich D, Ishida T, Oyama T*, et al.* Vascular endothelial growth factor inhibits the development of dendritic cells and dramatically affects the differentiation of multiple hematopoietic lineages in vivo. Blood 1998;92: 4150-66.
6. Kusmartsev S, Kusmartseva I, Afanasyev SG, Cherdyntseva NV. Immunosuppressive cells in bone marrow of patients with stomach cancer. Adv Exp Med Biol 1998;451: 189-94.
7. Bronte V, Chappell DB, Apolloni E*, et al.* Unopposed Production of Granulocyte-Macrophage Colony-Stimulating Factor by Tumors Inhibits CD8+ T Cell Responses by Dysregulating Antigen-Presenting Cell Maturation. J Immunol 1999;162: 5728-37.
8. Kusmartsev S, Li Y, Chen SH. Gr-1+ myeloid cells derived from tumor-bearing mice inhibit primary T cell activation induced through CD3/CD28 co-stimulation J Immunol 2000;165: 779-85.
9. Melani C, Chiodoni C, Forni G, Colombo MP. Myeloid cell expansion elicited by the progression of spontaneous mammary carcinomas in c-erbB-2 transgenic BALB/c mice suppresses immune reactivity." Blood Blood 2003;102: 2138-45.
10. Rodriguez PC, Hernandez CP, David Quiceno D*, et al.* Arginase I in myeloid suppressor cells is induced by COX-2 in lung carcinoma J Exp Med 2005;202: 931-9.
11. Sinha P, Clements VK, Fulton AM, Ostrand-Rosenberg S. Prostaglandin E2 promotes tumor progression by inducing myeloid-derived suppressor cells. Cancer Res 2007;67: 4507-13.
12. Rodriguez PC, Zea AH, Culotta KS, Zabaleta J, Ochoa JB, Ochoa AC. Regulation of T cell receptor CD3zeta chain expression by L-arginine. J Biol Chem 2002;277: 21123-29.
13. Bronte V, Serafini P, De Santo C*, et al.* IL-4-induced arginase 1 suppresses alloreactive T cells in tumor-bearing mice J Immunol 2003;170: 270-8.
14. Zea A, Rodriguez P, Atkins M*, et al.* Arginase-producing myeloid suppressor cells in renal cell carcinoma patients: a mechanism of tumor evasion. Cancer Res 2005;65: 3044-48.
15. Schmielau J, Finn OJ. Activated granulocytes and granulocyte-derived hydrogen peroxide are the underlying mechanism of suppression of t-cell function in advanced cancer patients." Cancer Res 2001;61: 4756-60.
16. Kusmartsev S, Gabrilovich DI. Inhibition of myeloid cell differentiation in cancer: The role of reactive oxygen species." J Leukoc Biol 2003;74: 186-96.
17. Huang B, Pan PY, Li Q*, et al.* Gr-1+CD115+ immature myeloid suppressor cells mediate the development of tumor-induced T regulatory cells and T-cell anergy in tumor-bearing host. Cancer Res 2006;66: 1123-31.
18. Kusmartsev S, Nagaraj S, Gabrilovich D. Tumor-associated CD8+ T cell tolerance induced by bone marrow-derived immature myeloid cells. J Immunol 2005;175: 4583-92.

19. Nagaraj S, Gupta K, Pisarev V*, et al.* Altered recognition of antigen is a mechanism of CD8+ T cell tolerance in cancer. Nat Med 2007;13(7): 828-35.
20. Su Z, Dannull J, Yang BK*, et al.* Telomerase mRNA-transfected dendritic cells stimulate antigen-specific CD8+ and CD4+ T cell responses in patients with metastatic prostate cancer. J Immunol 2005;174: 3798-807.
21. Dannull J, Su Z, Rizzieri D*, et al.* Enhancement of vaccine-mediated antitumor immunity in cancer patients after depletion of regulatory T cells. J Clin Invest 2005;115: 3623-33.
22. Almand B, Clark J, Nikitina E*, et al.* Increased production of immature myeloid cells in cancer patients. A mechanism of immunosuppression in cancer. J Immunol 2001;166: 678-89.
23. Kusmartsev S, Nefedova Y, Yoder D, Gabrilovich DI. Antigen-specific inhibition of CD8+ T cell response by immature myeloid cells in cancer is mediated by reactive oxygen species. J Immunol 2004;172: 989-99.
24. Angulo I, Rodriguez R, Garcia B, Medina M, Navarro J, Subiza JL. Involvement of nitric oxide in bone marrow-derived natural suppressor activity. Its dependence on IFN-gamma. J Immunol 1995;155: 15-26.
25. Mazzoni A, Bronte V, Visintin A*, et al.* Myeloid suppressor lines inhibit T cell responses by an NO-dependent mechanism. J Immunol 2002;168: 689-95.
26. Liu Y, Van Ginderachter J, Brys L, De Baetselier P, Raes G, Geldhof A. Nitric oxide-independent CTL suppression during tumor progression: association with arginase-producing (M2) myeloid cells. J Immunol 2003;170: 5064-74
27. Itoh Y, Ma FH, Hoshi H*, et al.* Determination and bioimaging method for nitric oxide in biological specimens by diaminofluorescein fluorometry. Anal Biochem 2000;287: 203-9.
28. Breitman TR, Chen ZX, Takahashi N. Potential applications of cytodifferentiation therapy in hematologic malignancies. Semin Hematol 1994;31: 18-25.
29. Mirza N, Fishman M, Fricke I*, et al.* All-trans-retinoic acid improves differentiation of myeloid cells and immune response in cancer patients. Cancer Res 2006;66: 9299-307.
30. Kusmartsev S, Cheng F, Yu B*, et al.* All-trans-retinoic acid eliminates immature myeloid cells from tumor-bearing mice and improves the effect of vaccination." Cancer Res 2003;63: 4441-49.
31. Malmberg KJ. Effective immunotherapy against cancer: a question of overcoming immune suppression and immune escape. Cancer Immunol Immunother 2004;53: 879-92.
32. Rivoltini L, Carrabba M, Huber V*, et al.* Immunity to cancer: attack and escape in T lymphocyte-tumor cell interaction. Immunol Rev 2002;188: 97-113.
33. Vieweg J, Su Z, Dahm P, Kusmartsev S. Reversal of tumor-induced immune suppression. Clin Cancer Res 2007;13 727-32.
34. Bronte V, Apolloni E, Cabrelle A*, et al.* Identification of a CD11b(+)/Gr-1(+)/CD31(+) myeloid progenitor capable of activating or suppressing CD8(+) T cells." Blood 2000; 96: 3838-

## FIGURE LEGENDS

**Figure 1. Characterization of $Lin^-HLA\text{-}DR^-$ myeloid cell population in peripheral blood of RCC patients. A**. MDSC were isolated from the PBMC of healthy donors and RCC patients (One representative pair of donor-patient from 9 are shown) by selecting lineage negative (CD3, CD14, CD19, CD56) and HLA-DR negative cells as described previously (22). **B.** Proportion of $Lin^-HLA\text{-}DR^-$ cells in peripheral blood of RCC patients is significantly increased. Freshly isolated PBMC from RCC patients and healthy donors were stained with CD3, CD14, CD19, CD56 and HLA-DR, and then analyzed by flow cytometry for presence of $Lin^-HLA\text{-}DR^-$ cell population. **C.** $Lin^-HLA\text{-}DR^-$ MDSC populations were characterized by flow cytometry. Cell surface marker expression is represented by the white histograms, while isotype controls are shown in the gray histograms.

**Figure 2. Isolation of $CD33^+HLA\text{-}DR^-$ MDSC populations**. **A**. PBMC obtained from a healthy volunteer and a RCC patient were labeled with anti-HLA-DR magnetic beads and subjected to magnetic separation. HLA-DR-negative cells were labeled with anti-CD33 magnetic beads and $CD33^+$ cells were isolated by positive selection. **A.** Whole PBMC and purified $CD33^+$ cells from RCC patient were stained with anti-CD33 and anti-CD11b or anti-CD114 antibody and then analyzed for cell surface marker expression by FACS **B.** Cytological analysis of $CD33^+HLA\text{-}DR^-$ cells. Cytospines with CD33-positive cells were prepared and stained with hematoxylin and eosin.

**Figure 3. RCC-derived $CD33^+HLA\text{-}DR^-$ cells inhibit T cell responses.**

**A**. ELISPOT assay. MDSC isolated from an HLA-A0201-positive healthy volunteer (Donor) or RCC patient (RCC) were pulsed with MART-1 peptide and incubated with a MART-1 specific CTL clone at a ratio of 1:1 for 20 h. Assay was developed as described in *Materials and Methods.* After washing, spots were counted using an automated ELISPOT counter. **B.** CTL assays were performed in the presence of MDSC isolated from an RCC patient as described in the legend to Figure 2B. We show that MDSC isolated from an RCC patient (RCC MDSC), but not from a healthy donor (Donor $CD33^+$ cells) inhibited cytolytic activity of MART-1-specifc CTL. Data were obtained from triplicates of single experiment representative of two. **C.** Effect of RCC-derived MDSC on tetanus toxoid (TT)-induced T cell proliferation. Dendritic cells derived from HLA-A0201-positive healthy volunteer were pulsed with tetanus toxoid (0.1 mg/ml of TT for 1 hour in 37$^o$C), washed and then cultured with autologous T cells (1:5) in round-bottomed 96-well plates for 4 days in presence or absence of RCC derived MDSC. [$^3$H]thymidine (1 μCi/well) was added 18 hours before cell harvest. Thymidine uptake was measured using a liquid scintill

**Figure 4. Involvement of ROS and NO in mechanisms of immune suppression mediated by $CD33^+HLA\text{-}DR^-$ cells.** To evaluate the role of ROS in MDSC-mediated immunosuppression catalase and/or superoxide dismutase (SOD), or uric acid were added to IFN-gamma ELISPOT assays in the presence of MDSC isolated from a RCC donor (**panel A**) and a healthy volunteer (**panel B**). MDSC isolated from an HLA-A0201-positive healthy volunteer (Donor) or RCC patient (RCC) were pulsed with MART-1 peptide and incubated with a MART-1 specific CTL clone at a ratio of 1:1 for 20 h. Assay was developed as described in Material and Methods. After washing, spots were counted using an automated ELISPOT counter. Antigen-specific

production of ROS and NO was measured by flow cytometry**.** MDSC were incubated with MART-1 specific clone, and after 1 hour, 5 μM of $H_2$DCFDA (**panel C**) or 5 μM DAF-FM diacetate (**panel D**) were added for 20 min. After washing, CD3-negative cells were analyzed by FACS (MDSC incubated with MART-1 specific CTL in the absence of fluorogenic probes are shown as grey histograms). Results of representative experiment out of two are shown.

**Figure 5.** RT-PCR analysis of RCC-derived myeloid-derived suppressor cells. Total RNA from dendritic cells (DC), HL-60 cell line, myeloid-derived suppressor cells (MDSC) and lineage-negative/ DR+ RCC-derived cells (Lin-/DR+) were isolated using TRIZOL reagent (Invitrogen). Reverse transcription was performed at 25°C for 10 min, 42°C for 2 h, and 72°C for 5 min from 100 ng of total RNA using Superscript II reverse transcriptase (Invitrogen) and random primers (3 μg/μl; Invitrogen).

**Figure 6. MDSC-mediated T cell inhibition in vitro can be reversed by ATRA**. **A**.CTL assays were performed in the presence of MDSC isolated from an RCC patient as described in the legend to Figure 2B. We show that MDSC isolated from an RCC patient (RCC MDSC), but not from a healthy donor (Donor MDSC) inhibited cytolytic activity of MART-1-specifc CTL. Exposure of MDSC to ATRA [1μM] was capable of abrogating the immunosuppressive function of $CD33^+HLA\text{-}DR^-$ MDSC (RCC MDSC+ATRA; Donor MDSC+ATRA). Data (Specific lysis percent ± SEM) are derived from triplicate wells of single experiment representative of 3. **B.** ATRA enhances in vitro differentiation of $CD33^+HLA\text{-}DR^-$ MDSC into APC**.** PBMC from an RCC patient were subjected to HLA-DR+ cell depletion, followed by positive selection for CD33. After 4 days of culture in GM-CSF-containing media supplemented without (**B, upper**

**panel**) or with 1μM ATRA (**B**, **lower panel**), the phenotype of isolated cells was analyzed by FACS.

**Figure 7**. **Treatment of patients with ATRA reduces immune suppressive potential of myeloid cells.** HLA-DR-negative, CD33-positive cells were isolated from a healthy donor and from RCC patients before (baseline) and after (post) treatment with Tretinoin (45 mg/m$^2$ daily for 7 days). Cells were added at varying numbers to co-cultures of MART-1 peptide-pulsed T2 cells and a MART-1-specific CTL clone. After 18 hours, culture supernatants were collected and analyzed for presence of IFN-gamma by ELISA. Data from healthy donor (**A**) and three RCC patients (**B, C, D**) are shown.